

2D Object Detection with Transformers: A Review

Tahira Shehzadi, Khurram Azeem Hashmi, Didier Stricker and Muhammad Zeshan Afzal

Abstract—Astounding performance of Transformers in natural language processing (NLP) has delighted researchers to explore their utilization in computer vision tasks. Like other computer vision tasks, DEtection TRansformer (DETR) introduces transformers for object detection tasks by considering the detection as a set prediction problem without needing proposal generation and post-processing steps. It is a state-of-the-art (SOTA) method for object detection, particularly in scenarios where the number of objects in an image is relatively small. Despite the success of DETR, it suffers from slow training convergence and performance drops for small objects. Therefore, many improvements are proposed to address these issues, leading to immense refinement in DETR. Since 2020, transformer-based object detection has attracted increasing interest and demonstrated impressive performance. Although numerous surveys have been conducted on transformers in vision in general, a review regarding advancements made in 2D object detection using transformers is still missing. This paper gives a detailed review of twenty-one papers about recent developments in DETR. We begin with the basic modules of Transformers, such as self-attention, object queries and input features encoding. Then, we cover the latest advancements in DETR, including backbone modification, query design and attention refinement. We also compare all detection transformers in terms of performance and network design. We hope this study will increase the researcher’s interest in solving existing challenges towards applying transformers in the object detection domain. Researchers can follow newer improvements in detection transformers on this webpage available at: https://github.com/mindgarage-shan/trans_object_detection_survey.

Index Terms—Detection Transformer, Deep Neural Networks, Self-attention, Object Detection, Computer Vision.

1 INTRODUCTION

Object detection is one of the fundamental tasks in computer vision that involves locating and classifying objects within an image [1], [2], [3], [4]. Over the years, convolutional neural networks (CNNs) have been the primary backbone for object detection models [1]. However, the recent success of transformers in natural language processing (NLP) has led researchers to explore their potential in computer vision as well [5]. The transformer architecture [6] has been shown to be effective in capturing long-range dependencies in sequential data [6], making it an attractive candidate for object detection tasks.

In 2020, Carion et al proposed a novel object detection framework called DEtection TRansformer (DETR) [7], which replaces the traditional region proposal-based methods with a fully end-to-end trainable architecture that uses a transformer encoder-decoder network. The DETR network showed promising results, outperforming traditional CNN-based object detectors [1], [2], [3], [4] while also eliminating the need for hand-crafted components such as region proposal networks and post processing steps such as non-maximum suppression (NMS) [8].

• All the members are with Department of Computer Science Technical University of Kaiserslautern, Mindgarage Lab, German Research Institute for Artificial Intelligence (DFKI) Kaiserslautern, Germany 67663
E-mail: Tahira.Shehzadi@dfki.de

Since the introduction of DETR, there have been several modifications and improvements proposed to overcome its limitations, such as slow training convergence and performance drops for small objects. Figure 1 shows the overview of the literature of the Detection Transformer (DETR) and its modifications to improve performance and training convergence. Deformable-DETR [9] modifies the attention modules to process the image feature map by considering the attention mechanism as the main reason for slow training convergence. UP-DETR [10] proposes a few modifications to Pre-train the DETR similar to pretraining transformers in natural language processing. Efficient-DETR [11] based on original DETR and Deformable-DETR examines the randomly initialized object probabilities, including reference points and object queries, which is one of the reasons for multiple training iterations. SMCA-DETR [12] introduces a Spatially-Modulated Co-attention module that replaces the existing co-attention mechanism in DETR to overcome the slow training convergence of DETR. TSP-DETR [13] deals with the cross-attention and the instability of bipartite matching to overcome the slow training convergence of DETR. Conditional-DETR [14] presents a conditional cross-attention mechanism to solve the training convergence issue of DETR. WB-DETR [15] considers CNN backbone for feature extraction as an extra component and presents a transformer encoder-decoder network without a

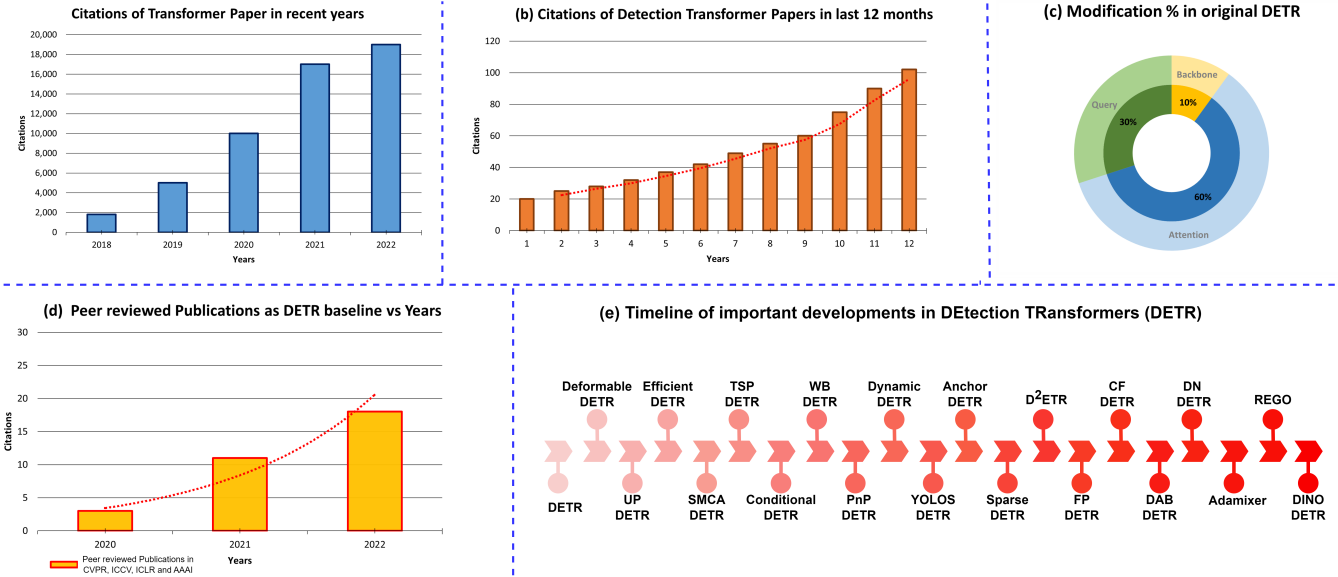


Fig. 1: Statistics overview of the literature on Transformers. (a) Number of citations per year of Transformer papers. (b) Citations in the last 12 months on Detection Transformer papers. (c) Modification percentage in original DEtection TRansformer (DETR) to improve performance and training convergence (d) Number of peer-reviewed publications per year that used DETR as a baseline. (e) A non-exhaustive timeline overview of important developments in DETR for detection tasks.

backbone. PnP-DETR [16] proposes a PnP sampling module to reduce spatial redundancy and make the transformer network computationally more efficient. Dynamic-DETR [17] introduces dynamic attention in the encoder-decoder network. YOLOS-DETR [18] presents the transferability and versatility of the Transformer from image recognition to detection in the sequence aspect using the least information about the spatial design of the input and improves performance. Anchor-DETR [19] proposes object queries as anchor points that are extensively used in CNN-based object detectors. Sparse-DETR [20] reduces computational cost by filtering encoder tokens with learnable cross-attention maps. D²ETR [21] uses the fine-fused feature maps in the decoder from backbone network with a novel cross-scale attention module. FP-DETR [22] reformulates the pretraining and fine-tuning stages for detection transformers. CF-DETR [23] refines the predicted locations by utilizing local information, as incorrect bounding box location reduces performance on small objects. DN-DETR [24] uses noised object queries as decoder additional input to reduce the instability of the bipartite-matching mechanism in DETR, which causes the slow convergence problem. AdaMixer [25] considers the encoder an extra network between the backbone and decoder that limits the performance and slower the training convergence because of its design complexity and proposes a 3D sampling process and few modifications in the decoder. REGO-DETR [26] proposes an ROI-based

method for detection refinement to improve the attention mechanism in the detection transformer. DINO [27] considers positive and negative noised object queries to make training convergence faster and to improve performance for small objects.

Due to the rapid progress of transformer-based detection methods, keeping track of new advancements is becoming increasingly challenging. Thus, a review of ongoing progress is necessary and would be helpful for the researchers in the field. This paper provides a detailed overview of recent advancements in 2D Detection Transformers. Table 1 shows the overview of modifications in Detection Transformer (DETR) to improve performance and training convergence.

1.1 Our Contributions

- 1) **Detailed review of transformer-based detection methods from architectural perspective.** We categorize and summarize improvements in DEtection TRansformer (DETR) according to Backbone modifications, pre-training level, attention mechanism, query design, etc. The proposed analysis aims to help researchers to have a more in-depth understanding of the key components of detection transformers in terms of performance indicators.
- 2) **A performance evaluation of detection transformers.** We evaluate improvements in detection trans-

TABLE 1: Overview of improvements in DEtection Transformer (DETR) to make training convergence faster and improve performance for small objects. Here, Bk represents backbone, Pre denotes Pre-training, Attn indicates Attention and Qry represents Query of transformer network. A description of the main contributions is shown here.

Methods	Bk	Pre	Modifications	Attn	Qry	Publication	Highlights
DETR [7]	-	-	-	-	-	ECCV 2020	Transformer, Set-based prediction, bipartite matching
Deformable-DETR [9]	-	-	-	✓	-	ICLR 2021	Deformable-attention module
UP-DETR [10]	-	✓	-	-	-	CVPR 2021	Unsupervised pre-training, random query patch detection
Efficient-DETR [11]	-	-	-	-	✓	arXiv 2021	Refence point and top-k queries selection module
SMCA-DETR [12]	-	-	-	✓	-	ICCV 2021	Spatially-Modulated Co-attention module
TSP-DETR [28]	-	-	-	✓	-	ICCV 2021	TSP-FCOS and TSP-RCNN modules for cross attention
Conditional-DETR [14]	-	-	-	-	✓	ICCV 2021	Conditional spatial queries
WB-DETR [15]	-	-	-	✓	-	ICCV 2021	Encoder-decoder network without a backbone, LIE-T2T encoder module
PnP-DETR [16]	-	-	-	✓	-	ICCV 2021	PnP sampling module including pool sampler and poll sampler
Dynamc-DETR [17]	-	-	-	✓	-	ICCV 2021	Dynamic attention in the encoder-decoder network
YOLOS-DETR [18]	-	-	-	✓	-	NeurIPS 2021	Pretraining encoder network
Anchor-DETR [19]	-	-	-	✓	✓	AAAI 2022	Row and Column decoupled-attention, object queries as anchor points
Sparse-DETR [20]	-	-	-	✓	-	ICLR 2022	Cross-attention map predictor, deformable-attention module
D^2 ETR [21]	-	-	-	✓	-	arXiv 2022	Fine fused features, cross-scale attention module
FP-DETR [22]	✓	✓	-	-	-	ICLR 2022	Multiscale tokenizer in place of CNN backbone, pretraining encoder network
CF-DETR [23]	-	-	-	✓	-	AAAI 2022	TEF module to capture spatial relationships, a coarse and a fine layer in the decoder network
DAB-DETR [29]	-	-	-	✓	-	ICLR 2022	Dynamic anchor boxes as object queries
DN-DETR [24]	-	-	-	✓	-	CVPR 2022	Positive noised object queries
AdaMixer [25]	-	-	-	✓	-	CVPR 2022	3D sampling module, Adaptive mixing module in the decoder
REGO [26]	-	-	-	✓	-	CVPR 2022	A multi-level recurrent mechanism and a glimpse-based decoder
DINO [27]	-	-	-	✓	-	arXiv 2022	Contrastive denoising module, positive and negative Noised object queries

formers using popular benchmark MS COCO [30]. We also highlight the advantages and limitations of these approaches.

- 3) **Analysis of accuracy and computational complexity of improved versions of detection transformers**
We present an evaluative comparison of state-of-the-art transformer-based detection methods w.r.t attention mechanism, backbone modification, query design improvement etc.
- 4) **Overview of key building blocks of detection transformers to improve performance further and future directions.** We examine the impact of various key architectural design modules that impact network performance and training convergence to provide possible suggestions for future research.

The remaining paper is arranged as follows. Section 2 discusses previous related surveys on transformers. Section 3 is related to object detection and transformers in all type of vision. Section 4 is the main part which explains the modifications in the DETR in details. Section 5 is about evaluation protocol and Section 6 provides evaluative comparison of detection transformers. Section 7 discusses open challenges and future directions. Finally, Section 8 concludes the paper.

2 RELATED PREVIOUS REVIEWS AND SURVEYS

Many surveys have studied deep learning approaches in 2D object detection [40], [41], [42], [43], [44], [45]. Table 2 lists

existing object detection surveys. Among these surveys, many studies comprehensively review approaches that process different 2D data types [31], [33], [46], [47]. Other studies focus on specific 2D applications [34], [48], [49], [50], [51], [52], [53], [54] and other tasks as segmentation [55], [56], [57], image captioning [58], [59], [60], [61] and object tracking [62]. Furthermore, some surveys examine deep learning methods and introduce vision transformers [36], [37], [38], [39]. However, most of the literature research were published before improvements in the detection transformer network, and a detailed review of transformer-based object detectors is missing. Thus, a survey of ongoing progress is necessary and would be helpful for researchers.

3 OBJECT DETECTION AND TRANSFORMERS IN VISION

3.1 Object Detection

This section explains the key concept of object detection and previously used object detectors. A more detailed analysis of object detection concepts can be found in [35], [63]. The object detection task localizes and recognizes objects in an image by providing a bounding box around each object and its category. These detectors are usually trained on datasets like PASCAL VOC [64] or MS COCO [30]. Backbone network extracts the features of input image as feature maps [65]. Usually, the backbone network such as the ResNet-50 [66] is pre-trained on ImageNet [67] and then finetuned

TABLE 2: Overview of previous surveys on object detection. For each paper, the publication details are provided.

Title	Year	Venue	Description
Advanced Deep-Learning Techniques for Salient and Category-Specific Object Detection: A Survey [31]	2018	SPM	It overviews different domains of object detection, i.e. objectness detection (OD), salient OD and category-specific OD.
Object Detection in 20 Years: A Survey [32]	2019	TPAMI	This work gives an overview of the evolution of object detectors.
Deep Learning for Generic Object Detection: A Survey [33]	2019	IJCV	A review on deep learning techniques on generic object detection.
A Survey on Deep Learning-based Architectures for Semantic Segmentation on 2D images [34]	2020	PRJ	Deep Learning-based methods for Semantic Segmentation are reviewed.
A Survey of Modern Deep Learning based Object Detection Models [35]	2021	ICV	It briefly overviews deep learning-based (regression-based single-stage and candidate-based two-stage) object detectors.
A Survey of Object Detection Based on CNN and Transformer [36]	2021	PRML	A review of the benefits and drawbacks of deep learning-based object detectors and introduction of transformer-based methods.
Transformers in computational visual media: A survey [37]	2021	CVM	It focuses on backbone design and low-level vision using vision transformer methods.
A survey: object detection methods from CNN to transformer [38]	2022	MTA	Comparison of various CNN-based detection networks and introduction of Transformer-based detection networks.
A Survey on Vision Transformer [39]	2023	TPAMI	This paper provides an overview of vision transformers and focuses on summarizing the state-of-the-art research in the field of Vision Transformers (ViTs).

to downstream tasks [68], [69], [70], [71]. Moreover, many works have also used visual transformers [72], [73], [74] as a backbone. Single-stage Object detectors [3], [4], [75], [76], [77], [78], [79], [80], [81], [82], [83] use only one network having faster speed but lower performance than two-stage networks. Two-stage object detectors [1], [2], [8], [65], [84], [85], [86], [87], [88], [89] contain two networks to provide final bounding boxes and class labels.

Lightweight Detectors: Lightweight detectors are a type of object detection models that are designed to be computationally efficient and require low computational resources compared to standard object detection models. These are real-time object detectors and can be employed on small devices. These networks include [90], [91], [92], [93], [94], [95], [96], [97], [98].

3D Object Detection: The primary purpose of 3D object detection is to recognize the objects of interest using a 3D bounding box and give a class label. 3D approaches are divided into three categories as image based [99], [100], [101], [102], [103], [104], [105], point cloud based [106], [107], [108], [109], [110], [111], [112], [113], [114] and multimodal fusion based [115], [116], [117], [118], [119].

3.2 Transformer for Segmentation

The self-attention mechanism can be employed for segmentation tasks [120], [121], [122], [123], [124] that provides pixel-level [125] prediction results. Panoptic segmentation [126] jointly solves semantic and instance segmentation tasks by providing per-pixel class and instance labels. Wang et al. [127] proposes location-sensitive axial attention for panoptic segmentation task on three benchmarks [128], [129], [130]. The above segmentation approaches have self-attention in CNN-based networks. Recently segmentation transformers [121], [123] are proposed containing encoder-decoder modules.

3.3 Transformers for Scene and Image Generation

Previously, text-to-image generation methods [131], [132], [133], [134] are based on GANs [135]. Ramesh et al. [136]

introduced a transformer-based model for generating high-quality images from provided text details. Transformer networks are also applied for image synthesis [137], [138], [139], [140], [141], which is important for learning unsupervised and generative models for downstream tasks. The feature learning with an unsupervised training procedure [138] achieves state-of-the-art performance on two datasets [142], [143], while SimCLR [144] provides comparable performance on [145]. The iGPT image generation network [138] does not include pre-training procedures similar to language modeling tasks. However, unsupervised CNN-based networks [146], [147], [148] consider prior knowledge as architectural layout, attention mechanism and regularization. Generative Adversarial Networks (GAN) [135] with CNN-based backbones have been appealing for image synthesis [149], [150], [151]. TransGAN [140] is a strong GAN network where the generator and discriminator contain transformer modules.

3.4 Transformers for Low-level Vision

Low-level vision is the process of analyzing images to identify their basic components and create an intermediate representation for further processing and higher-level tasks. After observing remarkable performance of attention networks in high-level vision tasks, many attention-based approaches have been introduced for low-level vision problems such as [152], [153], [154], [155], [156].

3.5 Transformers for Multi-Modal Tasks

Multi-Modal Tasks involve processing and combining information from multiple sources or modalities, such as text, images, audio, or video. The application of transformer networks in vision language tasks has also been widespread, including visual question-answering [157], visual commonsense-reasoning [158], cross-modal retrieval [159], and image captioning [160]. These transformer designs can be classified into single-stream [161], [162], [163], [164], [165], [166] and dual-stream networks [167], [168],

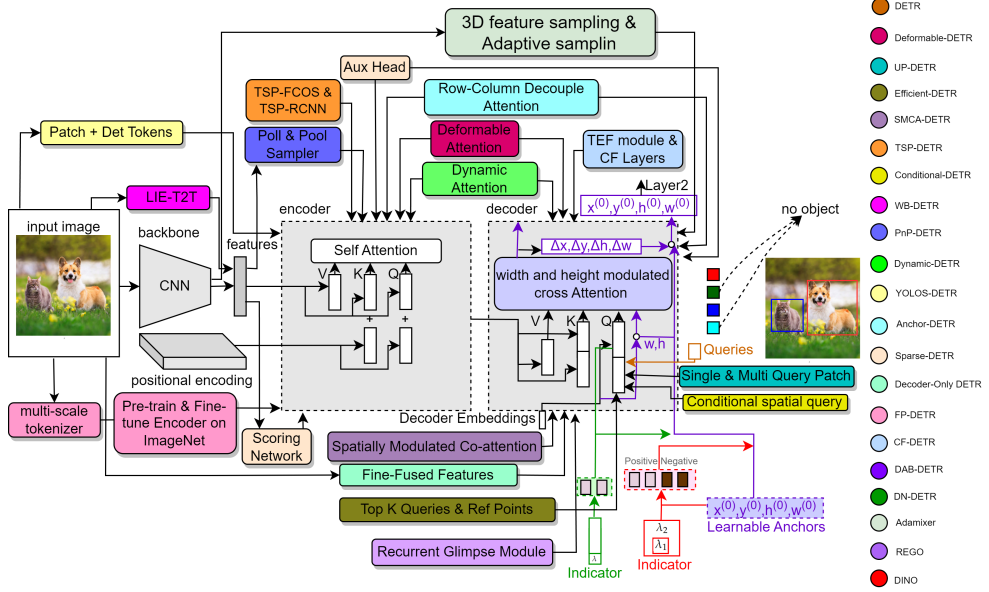


Fig. 2: An overview of the Detection Transformer (DETR) and its modifications proposed by recent methods to improve performance and training convergence. It considers the detection a set prediction task and uses the Transformer to free the network from post-processing steps such as non-maximal suppression (NMS). Here, each module added to DETR is represented with different color with its corresponding label(shown on the right side).

[169]. The primary distinction between these networks lies in the choice of loss functions.

4 DETECTION TRANSFORMERS

This section briefly explain DEtection TRansformer (DETR) and its improvements as shown in Figure 2.

4.1 DETR

DEtection TRansformer (DETR) [7] architecture is much simpler than CNN-based detectors like Faster R-CNN [170] as it removes the need for anchors generation process and post-processing steps such as non-maximal suppression (NMS) and provides an optimal detection framework. The DETR network has three main modules: a backbone network with positional encodings, an encoder and a decoder network with attention mechanism. The extracted features from the backbone network as one single vector and their positional encoding [171], [172] within the input vector fed to the encoder network. Here, the self-attention is performed on key, query and value matrices which feed to the multi-head attention and feed-forward network to find the attention probabilities of the input vector. The DETR decoder takes object queries in parallel with the encoder output. It computes predictions by decoding N number of object queries in parallel and uses a bipartite-matching

algorithm to label the ground truth and predicted objects as given in the following equation:

$$\hat{\sigma} = \arg \min_{\sigma \in N} \sum_k^N \mathcal{L}_m(y_k, \hat{y}_{\sigma(k)}), \quad (1)$$

Here, y_k is a set of ground truth (GT) objects. It provides boxes for both object and no object class, N is the total objects to be detected. Here, $\mathcal{L}_m(y_k, \hat{y}_{\sigma(k)})$ is the matching cost (for direct prediction) without duplicates between predicted objects with index $\sigma(k)$ and ground truth y_k as shown in the following equation:

$$\mathcal{L}_m(y_k, \hat{y}_{\sigma(k)}) = -\mathbb{1}_{\{c_k \neq \phi\}} \hat{p}_{\sigma(k)}(c_k) + \mathbb{1}_{\{c_k \neq \phi\}} \mathcal{L}_{bbox}(b_k, \hat{b}_{\sigma(k)}) \quad (2)$$

The next step is to compute the Hungarian loss by determining the optimal matching between ground truth (GT) and detected boxes regarding bounding-box region and label. The loss is reduced by Stochastic Gradient Descent (SGD).

$$\mathcal{L}_H(y, \hat{y}) = \sum_{k=1}^N [-\log \hat{p}_{\hat{\sigma}(k)}(c_k) + \mathbb{1}_{\{c_k \neq \phi\}} \mathcal{L}_{bbox}(b_k, \hat{b}_{\hat{\sigma}(k)})] \quad (3)$$

Where $\hat{p}_{\hat{\sigma}(k)}$ and c_k are the predicted class and target label, respectively, $\hat{\sigma}$ is the optimal-assignment factor, b_k and $\hat{b}_{\hat{\sigma}(k)}$ are ground-truth and predicted bounding-box, \hat{y} and $y = \{(c_k, b_k)\}$ are the prediction and ground truth of objects, respectively. Here, the bounding box loss is a linear combination of the generalized IoU (GIoU) loss [173] and of the L1 loss as shown in the following equation:

$$\mathcal{L}_{bbox} = \lambda_i \mathcal{L}_{iou}(b_k, \hat{b}_{\sigma(k)}) + \lambda_{l1} \| b_k - \hat{b}_{\sigma(k)} \|_1 \quad (4)$$

Where λ_i and λ_{l1} are the hyperparameters. DETR can only predict a fixed number of N objects in a single pass. For the COCO dataset, the value of N is set to 100 as this dataset has 80 classes. This network doesn't need NMS to remove redundant predictions as it uses bipartite matching loss with parallel decoding [174], [175], [176]. In comparison, previous work used RNNs-based autoregressive decoding [177], [178], [179], [180], [181]. The DETR network has several challenges, such as slow training convergence and performance drops for small objects. To address these challenges, modifications have been made to DETR network.

4.2 Deformable-DETR

The attention module of DETR provides a uniform weight value to all pixels of the input feature map at the initialization. These weights need many epochs for training convergence to find informative pixel locations. However, it requires high computation and extensive memory. The computation complexity of self-attention in encoder is $O(w_i^2 h_i^2 c_i)$, while the complexity of the cross-attention in decoder is $O(h_i w_i c_i^2 + N h_i w_i c_i)$. Here, h_i and w_i represent height and width of input feature map, respectively and N represents object queries fed as input the decoder. Let $q \in \Omega_q$ represent a query element with feature $z_q \in R^{c_i}$, and $k \in \Omega_k$ represents a key vector with feature $x_k \in R^{c_i}$, where c_i is the input features dimension, Ω_k and Ω_q indicate the set of key and query vectors, respectively. Then the feature of Multi-Head Attention (MHAtn) is computed by:

$$MHAtn(z_q, x) = \sum_{j=1}^J W_j [\sum_{k \in \Omega_k} A_{j q k} \cdot W'_j x_k] \quad (5)$$

where j represents the attention head, $W'_j \in R^{c_v \times c_i}$ and $W_j \in R^{c_i \times c_v}$ are of learnable weights ($c_v = c_i/J$ by default). The attention weights $A_{j q k} \propto \exp \frac{z_q^T U_j^T V_j x_k}{\sqrt{c_v}}$ are normalized as $\sum_{k \in \Omega_k} A_{j q k} = 1$, in which $U_j, V_j \in R^{c_v \times c_i}$ are also learnable weights. Deformable-DETR [9] modifies the attention modules inspired by [182], [183] to process the image feature map by considering the attention network as the main reason for slow training convergence and confined feature spatial resolution. This attention module works on taking a small number of samples nearby the reference point. Given an input feature map $x \in R^{c_i \times h_i \times w_i}$, let query q with content feature z_q and a 2d reference point r_q , the deformable attention feature is computed by:

$$DeformAttn(z_q, r_q, x) = \sum_{j=1}^J W_j [\sum_{k=1}^K A_{j q k} \cdot W_j x(r_q + \Delta r_{j q k})] \quad (6)$$

Where $\Delta r_{j q k}$ indexes the sampling offset. It takes ten times fewer training epochs than a simple DETR network. The complexity of self-attention becomes $O(w_i h_i c_i^2)$, which is linear complexity according to spatial size $h_i w_i$. The complexity of the cross-attention in decoder becomes $O(N K c_i^2)$ which is independent of spatial size $h_i w_i$. In Figure 3, the top right block indicates deformable attention module in Deformable-DETR.

Multi-Scale Feature Maps: High-resolution input image features increase the network efficiency, specifically for small objects. But, this is computationally expensive. Deformable-DETR provides high-resolution features without affecting the computation. It uses a feature pyramid containing high and low-resolution features rather than the original high-resolution input image feature map. This feature pyramid has an input image resolution of 1/8, 1/16 and 1/32 and contains its relative positional embeddings. In short, Deformable-DETR replaces the Transformer attention module in DETR with the multi-scale deformable attention module.

4.3 UP-DETR

Dai et al. [10] proposed a few modifications to pre-train the DETR similar to pre-training transformers in natural language processing. The random-sized patches from the input image are used as object queries to the decoder as input. The pretraining proposed by UP-DETR helps to detect these query patches from the input image. In Figure 3, the bottom left block denotes UP-DETR. Two issues are addressed during pretraining: multi-task learning and multi-query localization.

Multi-Task Learning: Object detection task combines object localization and classification, while these tasks always have distinct features [184], [185], [186]. The patch detection damages the classification features. Multi-task learning by patch feature reconstruction and a frozen pretraining backbone is proposed to protect the classification features of the transformer. The feature reconstruction is given as follows:

$$\mathcal{L}_{rec}(f_k, \hat{f}_{\hat{\sigma}(k)}) = \left\| \frac{f_k}{\|f_k\|_2} - \frac{\hat{f}_{\hat{\sigma}(k)}}{\|\hat{f}_{\hat{\sigma}(k)}\|_2} \right\|_2^2 \quad (7)$$

Here, the feature reconstruction term is \mathcal{L}_{rec} . It is the mean-squared error between l_2 (normalized) features of patches obtained from the CNN backbone.

Multi-query Localization: The decoder of DETR takes object queries as input to focus on different positions and box sizes. When this object queries number N (typically $N = 100$) is high, a single-query group is not suitable as it has convergence issues. To solve the multi-query localization problem between object queries and patches, UP-DETR proposes an attention mask and query shuffle mechanism. The number of object queries is divided into X different groups, where each query patch is provided to N/X object queries. These query patches are cropped randomly from the input image. Therefore, they are independent of each other. The Softmax layer of the self-attention module in the decoder is modified by adding attention mask inspired by [187] as follows:

$$P(q_i, k_i) = \text{Softmax} \left(\frac{q_i k_i^T}{\sqrt{d}} + \mathbf{M} \right) \cdot v_i \quad (8)$$

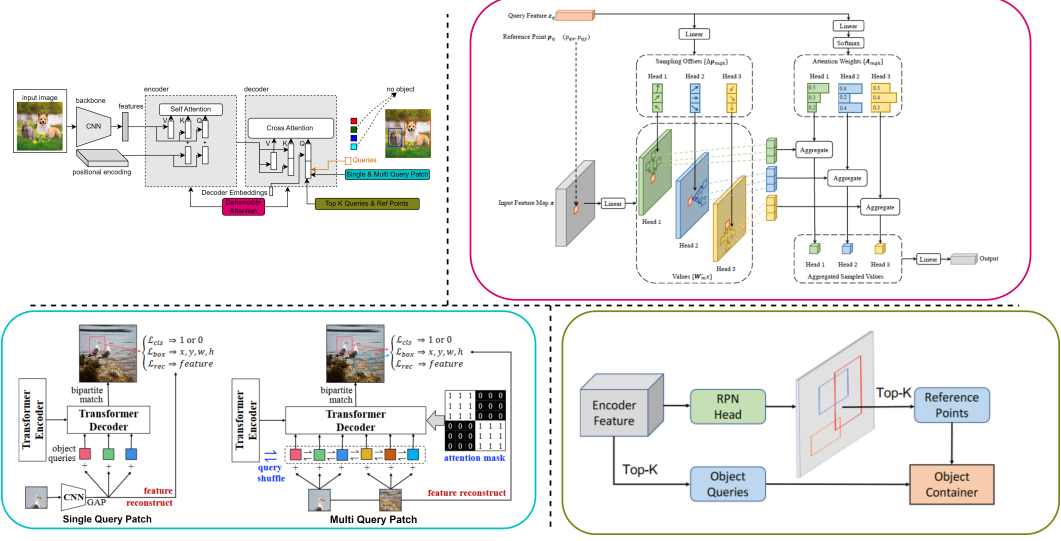


Fig. 3: The structure of the original DETR after the addition of Deformable-DETR [9], UP-DETR [10] and Efficient-DETR [11]. Here, the top left network is a simple DETR network, along with improvement indicated with small colored boxes. Larger boxes with corresponding colored borders are utilized to illustrate the internal mechanisms of these small colored boxes. The top right block indicates Deformable-DETR, the bottom left block indicates UP-DETR and the bottom right box represents Efficient-DETR (images from [9], [10], [11]).

$$M_{k,l} = \begin{cases} 0 & k, l \text{ in the same group} \\ -\infty & \text{otherwise} \end{cases} \quad (9)$$

Where $M_{k,l}$ is the interaction parameter of object query q_k and q_l . Though object queries are divided into groups, these queries don't have explicit groups during downstream training tasks. Therefore, during pre-training, these queries are randomly shuffled by masking 10% query patches to zero, similar to dropout [188].

4.4 Efficient-DETR

The performance of DETR also depends on the object queries as the detection head obtains final predictions from them. However, these object queries are randomly initialized at the start of training. Efficient-DETR [11] based on DETR and Deformable-DETR examines the randomly initialized object blocks, including reference points and object queries, which is one of the reasons for multiple training iterations. In Figure 3, the bottom right box shows Efficient-DETR.

Efficient-DETR has two main modules: a dense module and a sparse module. These modules have the same final detection head. The dense module includes the backbone network, encoder network and detection head. Following [189], It generates proposals by a class-specific dense prediction using the sliding window and selects Top-k features as object queries and reference points. Efficient-DETR uses 4-d boxes as reference points rather than 2d centres. The sparse network does the same work as the dense network, except

for their output size. The features from the dense module are taken as the initial state of the sparse module, which is considered a good initialization of object queries. Both dense and sparse module use one-to-one assignment rule as in [190], [191], [192].

4.5 SMCA-DETR

The decoder of the DETR takes object queries as input that are responsible for object detection in various spatial locations. These object queries combine with spatial features from the encoder. The co-attention mechanism in DETR involves computing a set of attention maps between the object queries and the image features to provide class labels and bounding box locations. However, the visual regions in the decoder of DETR related to object query might be irrelevant to the predicted bounding boxes. This is one of the reasons that DETR needs large number of training epochs to find suitable visual locations to identify corresponding objects correctly. Gao et al. [12] introduced a Spatially-Modulated Co-attention (SMCA) module that replaces the existing co-attention mechanism in DETR to overcome the slow training convergence of DETR. In Figure 4, the top right block represents SMCA-DETR. The object queries estimate the scale and center of its corresponding object, which are further used to set up a 2D spatial weight map. The initial estimate of scale l_h, l_w and center e_h, e_w of Gaussian-like

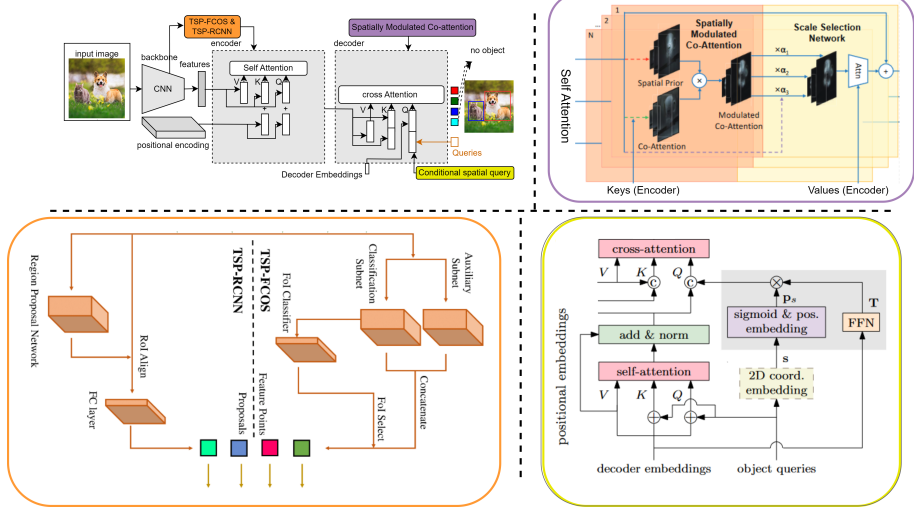


Fig. 4: The structure of the original DETR after the addition of SMCA-DETR [12], TSP-DETR [28] and Conditional-DETR [14]. Here, the top left network is a simple DETR network, along with improvement indicated with small colored boxes. Larger boxes with corresponding colored borders are utilized to illustrate the internal mechanisms of these small colored boxes. The top right block indicates SMCA-DETR, the bottom left block indicates TSP-DETR and the bottom right box represents Conditional-DETR (images from [12], [14], [28]).

distribution for object queries B_q is given as follows:

$$e_h^{nrm}, e_w^{nrm} = \text{sigmoid}(\text{MLP}(B_q)), \quad (10)$$

$$l_h, l_w = \text{FC}(B_q) \quad (11)$$

Where object query B_q provides a prediction center in normalized form by sigmoid activation function after two layers of MLP. These predicted centers are unnormalized to get center coordinates e_h, e_w in the input image. The object query also estimates the object scales as l_h, l_w . After the prediction of the object scale and center, SMCA provides a Gaussian-like weight map as follows:

$$\mathbf{W}(x, y) = \exp \left(-\frac{(x - e_w)^2}{\beta l_w^2} - \frac{(y - e_h)^2}{\beta l_h^2} \right) \quad (12)$$

Where β is the hyper-parameter to regulate the bandwidth, (x, y) is the spatial parameter of weight map \mathbf{W} . It provides high attention to spatial locations closer to the center and low attention to spatial locations away from the center.

$$A_i = \text{Softmax} \left(\frac{q_i k_i^T}{\sqrt{d}} + \log \mathbf{W} \right) v_i \quad (13)$$

Here, A_i is the co-attention map. The difference between the co-attention module in DETR and this co-attention module is the addition of the logarithm of the spatial-map \mathbf{W} . The decoder attention network has more attention near predicted box regions, which limits the search locations and thus converges the network faster.

4.6 TSP-DETR

TSP-DETR [13] deals with the cross-attention and the instability of bipartite matching to overcome the slow

training convergence of DETR. TSP-DETR proposes two modules based on an encoder network with feature pyramid networks (FPN) [65] to accelerate the training convergence of DETR. In Figure 4, the bottom left block indicates TSP-DETR. These modules are TSP-FCOS and TSP-RCNN, which used classical one-stage detector FCOS [193] and classical two-stage detector Faster-RCNN [194], respectively. TSP-FCOS used a new Feature of Interest (FoI) module to handle the multi-level features in the transformer encoder. Both modules use a bipartite matching mechanism to accelerate the training convergence.

TSP-FCOS: The TP-FCOS module follows the FCOS [193] for designing the backbone and FPN [65]. Firstly, the features extracted by the CNN backbone from the input image are fed to the FPN component to produce multi-level features. Two feature extraction heads, the classification head and auxiliary head, use four convolutional layers and group normalization [195], which are shared across the feature pyramid stages. Then, FoI classifier filters the concatenated output of these heads to select top-scored features. Finally, the transformer encoder network takes these FoIs and their positional encodings as input and provides class labels and bounding boxes as output.

TSP-RCNN: Like TP-FCOS, this module extracts the features by the CNN backbone and produces multi-level features by the FPN component. In place of two feature extraction heads used in TSP-FCOS, the TSP-RCNN module follows the design of Faster R-CNN [194]. It uses Region Proposal Network (RPN) to find Regions of Inter-

est (RoIs) to refine further. Each RoI in this module has an objectness score as well as a predicted bounding box. The RoIAlign [86] is applied on multi-level feature maps to take RoIs information. After passing through a fully connected network, these extracted features are fed to the Transformer encoder as input. The positional info of these RoI proposals is the four values $(c_{nx}, c_{ny}, w_n, h_n)$, where $(c_{nx}, c_{ny}) \in [0, 1]^2$ represents the normalized value of center and $(w_n, h_n) \in [0, 1]^2$ represents the normalized value of height and width. TSP-RCNN also used a set prediction loss during training. Finally, the transformer encoder network takes these RoIs and their positional encoding as input and predicts object labels and bounding boxes after passing through a shared feed-forward network.

4.7 Conditional-DETR

The cross-attention module in the DETR network highly depends on the quality of input embeddings to predict bounding boxes and class labels. The high-quality content embeddings increase the training convergence difficulty. Conditional-DETR [14] presents a conditional cross-attention mechanism to solve the training convergence issue of DETR. It differs from the simple DETR by input keys k_i and input queries q_i for cross-attention. In Figure 4, the bottom right box represents conditional-DETR. The conditional queries are obtained from 2D coordinates along with the embedding output of the previous decoder layer. The predicted candidate box from decoder-embedding is as follows:

$$box = \text{sig}(FFN(e) + [r^T 00]^T) \quad (14)$$

Here, e is the input embedding that is fed as input to the decoder. The box is a 4D vector $[box_{cx} \ box_{cy} \ box_w \ box_h]$, having the box center value as (box_{cx}, box_{cy}) , width value as box_w and height value as box_h . $\text{sig}()$ function normalizes the predictions varies from 0 to 1. $FFN()$ predicts the un-normalized box. r is the un-normalized 2D coordinate of the reference-point, and $(0, 0)$ is the simple DETR. This work either learns the reference point r for each box or generates them from the respective object query. It learns queries for multi-head cross-attention from input embeddings of the decoder. This spatial query makes the cross-attention head consider the explicit region, which helps to localize the different regions for class labels and bounding boxes by narrowing down the spatial range.

4.8 WB-DETR

DETR extracts local features by CNN backbone and gets global contexts by an encoder-decoder network of the transformer. WB-DETR [15] proves that the CNN backbone for feature extraction in detection transformers is not compulsory. It contains a transformer network without a backbone. It serializes the input image and feeds the local

features directly in each independent token to the encoder as input. The transformer self-attention network provides global information, which can accurately get the contexts between input image tokens. However, the local features of each token and the information between adjacent tokens need to be included as the transformer lacks the ability of local feature modeling. The LIE-T2T (Local Information Enhancement-T2T) module solves this issue by reorganizing and unfolding the adjacent patches and focusing on each patch's channel dimension after unfolding. In Figure 5, the top right block denotes the LIE-T2T module of WB-DETR. The iterative process of the LIE-T2T module is as follows:

$$P = \text{stretch}(\text{reshape}(P_i)) \quad (15)$$

$$Q = \text{sig}(e_2 \cdot \text{ReLU}(e_1 \cdot P)) \quad (16)$$

$$P_{i+1} = e_3 \cdot (P \cdot Q) \quad (17)$$

Where reshape function reorganize $(l_1 \times c_1)$ patches into $(h_i \times w_i \times c_i)$ feature-map. stretch denotes unfolding $(h_i \times w_i \times c_i)$ feature-map to $(l_2 \times c_2)$ patches. e_1 , e_2 and e_3 are the fully connected layer parameters. The ReLU activation is its nonlinear map function, and the sig generates final attention. The channel attention in this module provides local information as the relationship between the channels of the patches is the same as the spatial relation in the pixels of the feature map.

4.9 PnP-DETR

Transformer processes image feature maps that are transformed into a one-dimensional feature vector to produce the final results. Although effective, using the full feature map is expensive because of useless computation on background regions. PnP-DETR [16] proposes a poll and pool (PnP) sampling module to reduce spatial redundancy and make the transformer network computationally more efficient. This module divides the image feature map into background contextual features and fine foreground object features. Then, the transformer network uses these updated feature maps and translates them into the final detection result. In Figure 5, the bottom left block indicates PnP-DETR. This PnP Sampling module includes a pool sampler and a poll sampler, as explained below.

Poll Sampler: The poll sampler provides fine feature vectors V_f . A meta-scoring module is used to find the informational value for every spatial location (x, y) :

$$a_{xy} = \text{ScoreNet}(v_{xy}, \theta_s) \quad (18)$$

The score value is directly related to the information of feature vector f_{xy} . These score values are sorted as follows:

$$[a_z, |z = 1, \dots, Z|], \aleph = \text{Sort}(a_{xy}) \quad (19)$$

Where $Z = h_i w_i$ and \aleph is the sorting-order. The top N_s -scoring vectors are selected to get fine features:

$$V_f = [v_z, |z = 1, \dots, N_s] \quad (20)$$

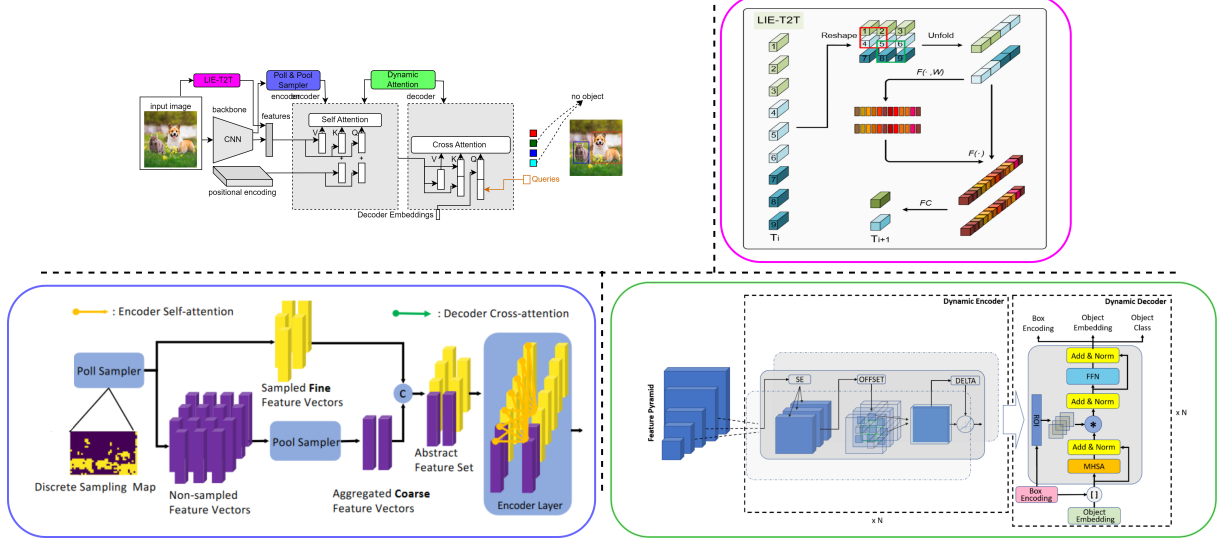


Fig. 5: The structure of the original DETR after the addition of WB-DETR [15], PnP-DETR [16] and Dynamic-DETR [17]. Here, the top left network is a simple DETR network, along with improvement indicated with small colored boxes. Larger boxes with corresponding colored borders are utilized to illustrate the internal mechanisms of these small colored boxes. The top right block indicates WB-DETR, the bottom left block indicates PnP-DETR and the bottom right box represents Dynamic-DETR (images from [15], [16], [17]).

Here, the predicted informative value is considered as a modulating factor to sample the fine feature vectors:

$$\mathbb{V}_f = [v_z \times a_z, |z = 1, \dots, N_s] \quad (21)$$

To make the learning stable, the feature vectors are normalized:

$$\mathbb{V}_f = [L_{norm}(v_z) \times a_z, |z = 1, \dots, N_s] \quad (22)$$

Here, L_{norm} is the layer normalization, $N_s = \alpha Z$, where α is the poll ratio factor. This sampling module reduces the training computation.

Pool Sampler: The poll sampler gets the fine features of foreground objects. A pool sampler compresses the remaining feature vectors of the background region that provides contextual information. It performs weighted pooling to get a small number M_b of background features motivated by double attention operation [196] and bilinear pooling [197]. The remaining feature vectors of the background region are:

$$\mathbb{V}_b = \mathbb{V} \setminus \mathbb{V}_f = \{\mathbf{v}_b, |b = 1, \dots, Z - N\} \quad (23)$$

The aggregated weights $\mathbf{a}_b \in \mathbb{R}^{M_b}$ are obtained by projecting the features with weight values $\mathbf{w}^s \in \mathbb{R}^{c_i \times M_b}$ as:

$$\mathbf{a}_b = \mathbf{v}_b \mathbf{w}^s \quad (24)$$

The projected features with learnable weight $\mathbf{w}^p \in \mathbb{R}^{c_i \times c_i}$ are obtained as follows:

$$\mathbf{v}_b = \mathbf{v}_b \mathbf{w}^p \quad (25)$$

The aggregated weights are normalized over the non-sampled regions with Softmax as follows:

$$a_{bm} = \frac{e_{bm}^a}{\sum_{b=1}^{N-Z} e^a b m} \quad (26)$$

By using the normalized aggregation weight, the new feature vector is obtained that provides information of non-sampled regions:

$$\mathbf{v}_m = \sum_{b=1}^{Z-N} \mathbf{v}_b \times a_{bm} \quad (27)$$

By considering all Z aggregation weights, the coarse background contextual feature vector is as follows:

$$\mathbf{V}_c = \{\mathbf{v}_m, |b = 1, \dots, M_b\} \quad (28)$$

The pool sampler provides context information at different scales using aggregation weights. Here, some feature vectors may provide local context while others may capture global context.

4.10 Dynamic-DETR

Dynamic-DETR [17] introduces dynamic attention in the encoder-decoder network of DETR to solve the slow training convergence issue and detection of small objects. Firstly, a convolutional dynamic encoder is proposed to have different attention types to the self-attention module of the encoder network to make the training convergence faster. The attention of this encoder depends on various factors such as spatial effect, scale effect and input feature

dimensions effect. Secondly, ROI-based dynamic attention is replaced with cross-attention in the decoder network. This decoder helps focus on small objects, reduces learning difficulty and converges the network faster. In Figure 5, the bottom right box represents Dynamic-DETR. This dynamic encoder-decoder network is explained in detail as follows.

Dynamic Encoder: The Dynamic-DETR uses a convolutional approach for the self-attention module. Given the feature vectors $F = \{F_1, \dots, F_n\}$, where $n=5$ represents object detectors from the feature pyramid, the multi-scale self-attention (MSA) is as follows:

$$Attn = MSA(F).F \quad (29)$$

However, it is impossible because of the various scale feature map from the FPN. For this, the feature maps of different scales are equalized within neighbours using 2D convolution as in the Pyramid Convolution [198] as follows:

$$F_i^+ = \{Upsample(DeformConv(F_{i-1}, l_i)), \\ DeformConv(F_i, l_i), \quad (30)$$

$$Downsample(DeformConv(F_{i+1}, l_i))\} \\ l_i = Offset(F_i) \quad (31)$$

Here, deformable convolution is applied to approximate self-attention in the spatial domain because simple convolution has a small kernel size. It focuses on spatial locations of the un-resized mid-layer and transfers information to its scaled neighbours. Moreover, SE [199] is applied for combining the features to provide scale attention:

$$w^{F_i} = SE(F_i^+) \quad (32)$$

Then, dynamic ReLU [200] is applied to get attention representation channel or feature dimension:

$$DynReLU(x_r) = \max(p_r^1 x_r + q_r^1, p_r^2 x_r + q_r^2) \quad (33)$$

$$p_r^1, q_r^1, p_r^2, q_r^2 = Delta(x_r) \quad (34)$$

Finally, the multi-scale self-attention (MSA) is formulated as follows:

$$MSA(P) = \text{Concat}_{i=1 \dots k}(DynReLU(w^{F_i} F_i^+)) \quad (35)$$

The attention of the dynamic encoder as in [201] depends on various factors such as spatial effect, scale effect and input feature dimensions effect.

Dynamic Decoder: The dynamic decoder uses mixed attention blocks in place of multi-head layers to ease the learning in cross-attention network and improves the detection of small objects. It also uses dynamic convolution in place of a cross-attention layer inspired by ConvBERT [202] in natural language processing (NLP). Firstly, ROI Pooling [194] is introduced in the decoder network. Then position embeddings are replaced with box encoding $BE \in \mathbb{R}^{p \times 4}$ as the image size. The output from the dynamic encoder, along with box encoding BE is fed to the dynamic decoder to

pool image features $R \in \mathbb{R}^{p \times s \times s \times c_i}$ from feature pyramid as follows:

$$R = RoI_{pool}(F_{encoder}, BE, s) \quad (36)$$

where s is the size of pooling parameter, c_i represents quantity of channels of $F_{encoder}$. To feed this in the cross-attention module, input embeddings $qe \in \mathbb{R}^{p \times c_i}$ are required for object queries. These embeddings are passed through the Multi-Head self Attention (MHSAttn) layer as:

$$qe^* = MHSAttn(qe, qe, qe) \quad (37)$$

Then these query embeddings are passed through fully-connected layer (dymaic filters) as follows:

$$Filter^{qe} = FC(qe^*) \quad (38)$$

Finally, cross-attention between features and object queries is performed with 1×1 convolution using dynamic filters $Filter^{qe}$:

$$qe^F = Con_{1 \times 1}(F, Filter^{qe}) \quad (39)$$

These features are passed through the FFN layers to provide the various prediction as updated object-embedding, updated box-encoding and the object class. This process eases the learning of the cross-attention module by focusing on sparse areas and then spreading to global regions.

4.11 YOLOS-DETR

Vision Transformer (ViT) [5] inherited from NLP performs well on the image recognition task. ViT-FRCNN [203] uses a pre-trained backbone (ViT) for a CNN-based detector. It utilizes convolution neural networks and relies on strong 2D inductive biases and region-wise pooling operations for object-level perception. Other similar works as DETR [7], introduce 2D inductive bias by using CNNs and pyramidal features. YOLOS-DETR [18] presents the transferability and versatility of the Transformer from image recognition to detection in the sequence aspect using least information about the spatial design of the input. It closely follows ViT architecture with two simple modifications. Firstly, it removes the image-classification patches [CLS] and adds randomly initialized one hundred detection patches [DET] as [204] along with the input patch embeddings for object detection. Secondly, similar to DETR a bipartite matching loss is used in place of ViT classification loss. The transformer encoder takes the generated sequence as input as follows:

$$s_0 = [I_p^1 L; \dots; I_p^M L; I_d^1; \dots; I_d^{100}] + PE \quad (40)$$

Where, I is the input image $I \in \mathbb{R}^{h_i \times w_i \times c_i}$ that is reshaped into 2D tokens $I_p \in \mathbb{R}^{n_i \times (R^2 \cdot c_i)}$. Here, h_i represents height and w_i indicates width of input image. c_i is the total channels. (r, r) is each token resolution, $n_i = \frac{h_i w_i}{r^2}$ is the total number of tokens. These tokens are mapped to D_i dimensions with linear projection $L \in \mathbb{R}^{(r^2 \cdot c_i) \times D_i}$. The result of this projection is $I_p L$. The encoder also takes randomly

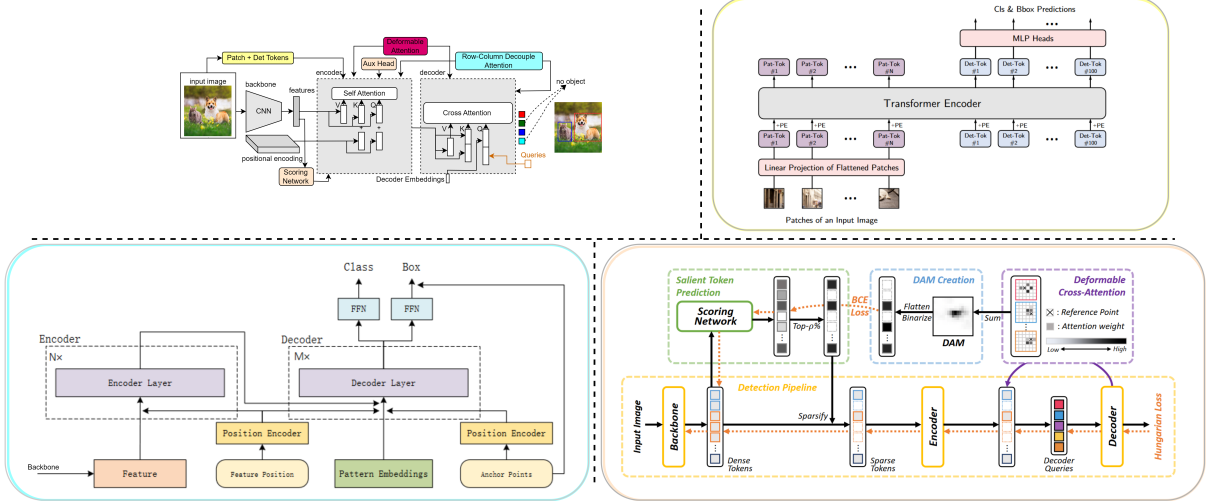


Fig. 6: The structure of the original DETR after the addition of YOLOS-DETR [18], Anchor-DETR [19] and Sparse-DETR [20]. Here, the top left network is a simple DETR network, along with improvement indicated with small colored boxes. Larger boxes with corresponding colored borders are utilized to illustrate the internal mechanisms of these small colored boxes. The top right block indicates YOLOS-DETR, the bottom left block indicates Anchor-DETR and the bottom right box represents Sparse-DETR (images from [18], [19], [20]).

initialized one hundred learnable tokens $\mathbf{I}_d \in \mathbb{R}^{100 \times D_i}$. To keep the positional information, positional embeddings $\mathbf{PE} \in \mathbb{R}^{(n_i+100) \times D_i}$ are also added. The encoder of transformer contains multi-head self-attention mechanism and one MLP block with GELU [205] non-linear activation function. The Layer Normalization (LN) [206] is added between each self-attention and MLP block as follows:

$$\dot{s}_n = MHSAttn(LN(s_{n-1})) + s_{n-1} \quad (41)$$

$$s_n = MLP(LN(\dot{s}_n)) + \dot{s}_n \quad (42)$$

Where s_n is the encoder input sequence. In Figure 6, the top right block indicates YOLOS-DETR.

4.12 Anchor-DETR

DETR uses learnable embeddings as object queries in the decoder network. These input embeddings do not have a clear physical meaning and cannot illustrate where to focus. It is challenging to optimize the network as object queries do not focus on the specific regions. Anchor-DETR [19] solves this issue by proposing object queries as anchor points that are extensively used in CNN-based object detectors. This query design can provide multiple object predictions at one region. Moreover, a few modifications in the attention are proposed that reduce the memory cost and improve performance. In Figure 6, the bottom left block shows Anchor-DETR. The two main contributions of Anchor-DETR: query and attention variant design, are explained as follows.

Anchor Points as Object Queries: The CNN-based object detectors consider anchor points as the relative position

of the input feature maps. In contrast, transformer-based detectors take uniform grid locations, hand-craft locations or the learned locations as anchor points. Anchor-DETR considers two types of anchor points: learned anchor locations and grid anchor locations. The grid anchor locations are input image grid points. The learned anchor locations are uniform distributions from 0 to 1 (randomly initialized) and updated using the learned parameters.

Row and Column Decoupled-Attention: DETR requires huge GPU memory as in [207], [208] because of the complexity of the cross-attention module. It is more complex than the self-attention module in the decoder. Although Deformable-DETR reduces memory cost, it still causes random memory access, making the network slower. Row-Column Decoupled Attention (RCDA), as shown in the bottom left block of Figure 6, reduces memory and provides similar or better efficiency.

4.13 Sparse-DETR

Sparse-DETR [20] filters the encoder tokens by learnable cross-attention map predictor. After distinguishing these tokens in the decoder network, it focuses only on foreground tokens to reduce computational costs.

Sparse-DETR introduces the scoring module, aux-heads in the encoder and the Top-k queries selection module for the decoder. In Figure 6, the bottom right box represents Sparse-DETR. Firstly, it determines the saliency of tokens, fed as input to the encoder, using the scoring network that selects top $\rho\%$ tokens. Secondly, the aux-head takes the top-k tokens from the output of the encoder network. Finally,

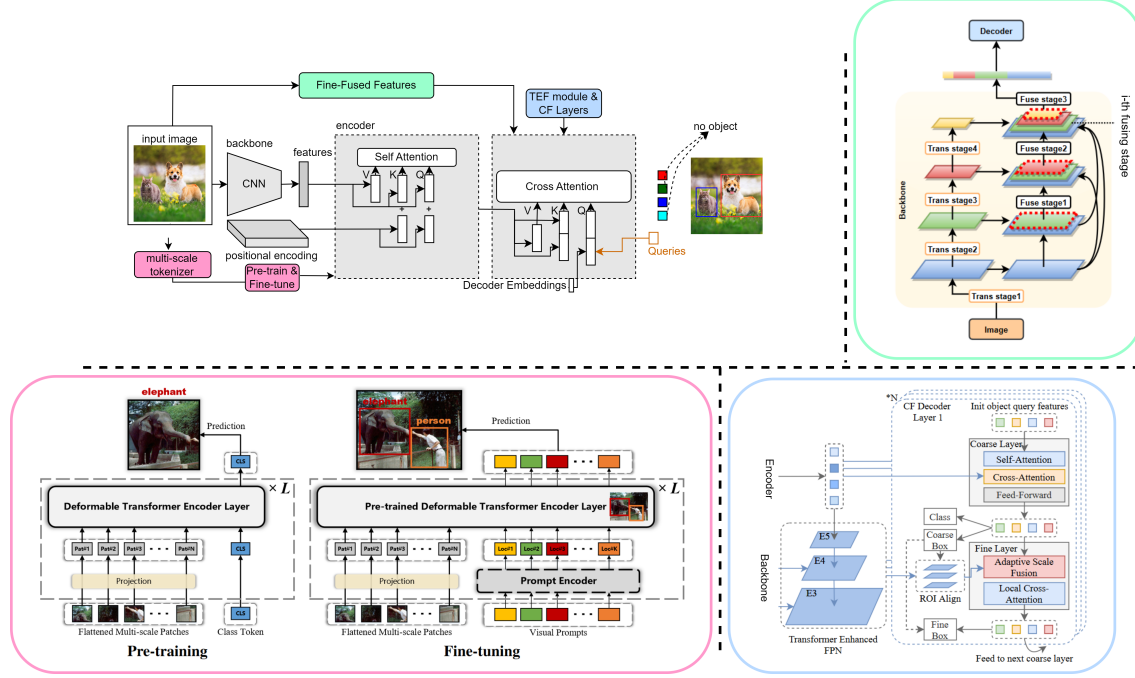


Fig. 7: The structure of the original DETR after the addition of D²ETR [21], FP-DETR [22] and CF-DETR [23]. Here, the top left network is a simple DETR network, along with improvement indicated with small colored boxes. Larger boxes with corresponding colored borders are utilized to illustrate the internal mechanisms of these small colored boxes. The top right block indicates D²ETR, the bottom left block indicates FP-DETR and the bottom right box represents CF-DETR (images from [21], [22], [23]).

the top- k tokens are used as the decoder object queries. The salient token prediction module refines encoder tokens that are taken from the backbone feature map using threshold ρ and update the features $x_l - 1$ as:

$$\mathbf{x}_l^m = \begin{cases} x_{l-1}^m & m \notin \Omega_r^q \\ LN(FFN(y_l^m) + y_l^m) & m \in \Omega_r^q, \end{cases}$$

where $y_l^m = LN(DeformAttn(x_{l-1}^m, x_{l-1}) + x_{l-1}^m)$ (43)

Where DeformAttn is the deformable attention, FFN is the Feed-Forward Network, and LN is the Layer-Normalization. Then, the Decoder Cross-Attention Map (DAM) accumulates the attention weights of decoder object queries, and the network is trained by minimizing loss between prediction and binarized DAM as follows:

$$\mathcal{L}_{dam} = \frac{-1}{M} \sum_{k=1}^M BCELoss(sn(x_f), DAM_k^b) \quad (44)$$

Where BCELoss is the binary cross-entropy (BCE) loss, DAM_k^b is the k th binarized DAM value of the encoder token, and sn is the scoring network. In this way, sparse-DETR minimizes the computation by significantly eliminating encoder tokens.

4.14 D²ETR

Much work [9], [11], [12], [13], [14] has been proposed to make the training convergence faster by modifying the cross-attention module. Many researchers [9] used multi-scale feature maps to improve performance for small objects. However, the solution for high computation complexity has yet to be proposed. D²ETR [21] achieves better performance with low computational cost. Without an encoder module, the decoder directly uses the fine-fused feature maps provided by the backbone network with a novel cross-scale attention module. The D²ETR contains two main modules a backbone and a decoder. The backbone network based on Pyramid Vision Transformer (PVT) consists of two parallel layers, one for cross-scale interaction and another for intra-scale interaction. This backbone contains four transformer levels to provide multi-scale feature maps. All levels have the same architecture depending on the basic module of the selected Transformer. The backbone also contains three fusing levels in parallel with four transformer levels. These fusing levels provide a cross-scale fusion of input features. The i -th fusing level is shown in the top right block of Figure 7. The cross-scale attention is formulated as follows:

$$f_j = \mathbf{L}_j(f_{j-1}) \quad (45)$$

$$f_j^* = SA(f_q, f_k, f_v) \quad (46)$$

$$f_q = f_j, f_k = f_v = [f_1^*, f_2^*, \dots, f_{j-1}^*, f_j] \quad (47)$$

where f_j^* the fused form feature map f_j . Given that L is the input of the decoder as the last-level feature map, the final result of cross-scale attention is $f_1^*, f_2^*, \dots, f_L^*$. The output of this backbone is fed to the decoder that takes object queries in parallel. It provides output embeddings independently transformed into class labels and box coordinates by a forward feed network. Without an encoder module, the decoder directly used the fine-fused feature maps provided by the backbone network with a novel cross-scale attention module providing better performance with low computational cost.

4.15 FP-DETR

Modern CNN-based detectors like YOLO [209] and Faster-RCNN [194] utilize specialized layers on top of backbones pre-trained on ImageNet to enjoy pre-training benefits such as improved performance and faster training convergence. DETR network and its improved version [10] only pre-train its backbone while training from scratch both encoder and decoder layers. Thus, the transformer needs massive training data for fine-tuning. The main reason for not pre-train the detection transformers is the difference between the pre-training and final detection tasks. Firstly, The decoder module of the transformer takes multiple object queries as input for detecting objects, while ImageNet classification takes only a single query (class token). Secondly, the self-attention module and the projections on input query embeddings in the cross-attention module easily overfit a single class query, making the decoder network difficult to pre-train. Moreover, the downstream detection task focuses on classification and localization, while the upstream task considers only classification for the objects of interest.

FP-DETR [22] reformulates the pre-training and fine-tuning stages for detection transformers. In Figure 7, the bottom left block indicates FP-DETR. It takes only the encoder network of the detection transformer for pre-training as it is challenging to pre-train the decoder on the ImageNet classification task. Moreover, DETR uses both the encoder and CNN backbone as feature extractors. FP-DETR replaces the CNN backbone with a multi-scale tokenizer and uses the encoder network to extract features. It fully pre-trains the Deformable-DETR on the ImageNet dataset and fine-tunes it for final detection that achieves competitive performance.

4.16 CF-DETR

CF-DETR [23] observes that COCO-style metric Average Precision (AP) results for small objects on detection transformers at low IoU threshold values are better than CNN-based detectors. It refines the predicted locations by utilizing local information, as incorrect bounding box location

reduces performance on small objects. In Figure 7, the bottom right box represents CF-DETR. It introduces the Transformer Enhanced FPN (TEF) module, coarse layers and fine layers in the decoder network of DETR. The TEF module provides the same functionality as FPN, has non-local features E4 and E4 extracted from the backbone and E5 features taken from the encoder output. The features of the TEF module and encoder network are fed to the decoder as input. The decoder modules introduce a coarse block and a fine block. The coarse block selects foreground features from the global context. The fine block has two modules as Adaptive Scale-Fusion (ASF) and Local Cross-Attention (LCA) which further refine coarse boxes.

4.17 DAB-DETR

DAB-DETR [29] uses the bounding box coordinates as object queries in the decoder and gradually updates them in every layer. In Figure 8, the top right block indicates DAB-DETR. These box coordinates make training convergence faster by providing positional information and using the height and width values to update the positional attention map. This type of object query provides better spatial prior for the attention mechanism and provides a simple query formulation mechanism.

The decoder network needs keys k_i , queries q_i and values v_i having two main networks a self-attention network to update queries and a cross-attention network to find features probing. Given a bounding box coordinates $Anchor_i = (x_i, y_i, w_i, h_i)$ as object queries in the decoder with content-query C_i , its positional-query P_i is formed as follows:

$$P_{q_i} = MLP(PE_i(Anchor_i)) \quad (48)$$

$$PE_i(A_q) = Conc(PE_i(x_q), PE_i(y_q), PE_i(w_q), PE_i(h_q)) \quad (49)$$

Where PE_i is the positional encoding that contains information about the absolute or relative position of input features. Here, MLP has a linear layer and ReLU non-linear function for extracting the features. The difference between the self-Attention of original DETR and DAB-DETR is that query, and key matrices has also position information taken from bounding-box coordinates. The cross-attention module concatenates the position and content information in queries and keys matrices and determines their corresponding heads. The decoder takes input embeddings as content queries and anchor boxes as positional queries to find object probabilities related to anchors and content queries. This way, dynamic box coordinates used as object queries make training convergence faster and increase detection results for small objects.

4.18 DN-DETR

DN-DETR [24] uses noised object queries as decoder additional input to reduce the instability of the bipartite-

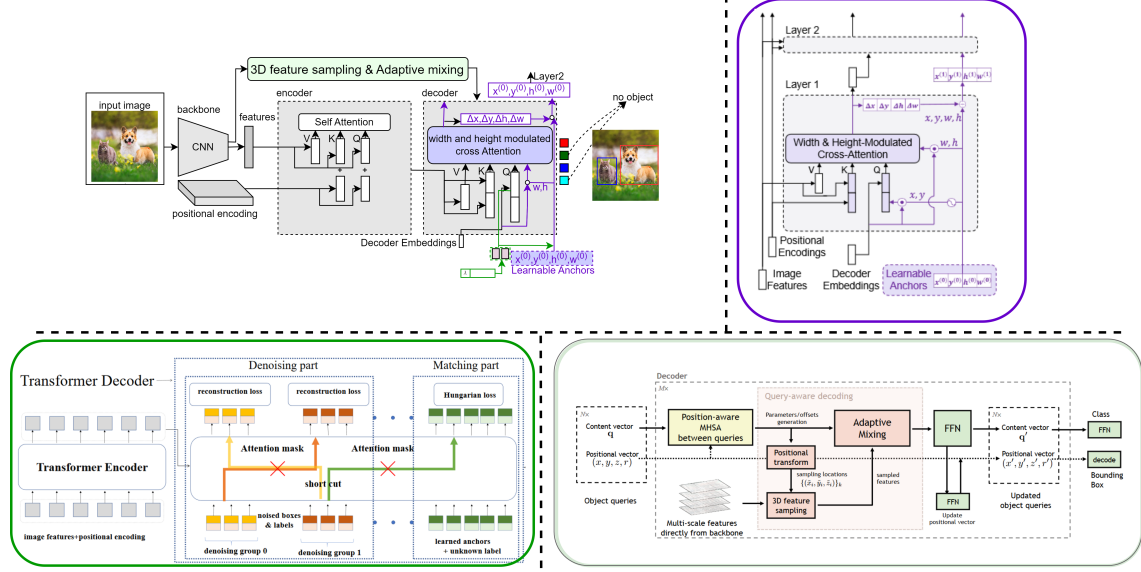


Fig. 8: The structure of the original DETR after the addition of DAB-DETR [29], DN-DETR [24] and AdaMixer [25]. Here, the top left network is a simple DETR network, along with improvement indicated with small colored boxes. Larger boxes with corresponding colored borders are utilized to illustrate the internal mechanisms of these small colored boxes. The top right block indicates DAB-DETR, the bottom left block indicates DN-DETR and the bottom right box represents AdaMixer (image from [24], [25], [29]).

matching mechanism in DETR, which causes the slow convergence problem. In Figure 8, the bottom left block indicates DN-DETR. The decoder queries have two parts: the denoising part containing noised ground-truth box-label pairs as input and the matching part containing learnable anchors as input. The matching part $M = \{M_0, M_1, \dots, M_{l-1}\}$ determines the resemblance between the ground-truth label pairs and the decoder output, while the denoising part $d = \{d_0, d_1, \dots, d_{k-1}\}$ attempts to reconstruct the ground-truth objects as:

$$\text{Output} = \text{Decoder}(d, M, I|A) \quad (50)$$

Where I is the image features taken as input from the transformer encoder, and A is the attention mask that stops the information transfer between the matching and denoising parts and among different noised levels of the same ground truth objects. The decoder has noised levels of ground-truth objects where noise is added to bounding boxes and class labels, such as label flipping. It contains a hyperparameter λ for controlling the noise level. The training architecture of DN-DETR is based on DAB-DETR, as it also takes bounding box coordinates as object queries. The only difference between these two architectures is the class label indicator as an additional input in the decoder to assist label denoising. The bounding boxes are updated inconsistently in DAB-DETR, making relative offset learning challenging. The denoising module in DN-DETR bypasses the bipartite matching process and simplifies relative offset learning.

4.19 AdaMixer

AdaMixer [25] considers the encoder an extra network between the backbone and decoder that limits the performance and slower the training convergence because of its design complexity. In Figure 8, the bottom right box represents AdaMixer. The main modules of AdaMixer are explained as follows.

3D feature space For 3D feature space, input feature map from the CNN backbone with the downsampling stride s_i^f , is first transformed by a linear-layer to the same d_f channel and computed the coordinate of its z-axis as follows:

$$z_i^f = \log_2(s_i^f / s_b). \quad (51)$$

Where, the height h_i and width w_i of feature-maps (different strides) is rescaled to h_i/s_b and w_i/s_b , where $s_b = 4$.

3D feature sampling process In the sampling process, query generates I_p groups of vectors to I_p points, $(\Delta x_j, \Delta y_j, \Delta z_j)_{I_p}$, where each vector is dependent on its content-vector q_i by a linear-layer L_i as follows:

$$(\Delta x_j, \Delta y_j, \Delta z_j)_{I_p} = L_i(q_i). \quad (52)$$

These offset values are converted into sampling positions w.r.t position vector of object query as follows:

$$\begin{cases} \tilde{x}_j = x + \Delta x_j \cdot 2^{z-r} \\ \tilde{y}_j = y + \Delta y_j \cdot 2^{z+r}, \\ \tilde{z}_j = z + \Delta z_j, \end{cases} \quad (53)$$

The interpolation over the 3D feature space first samples by

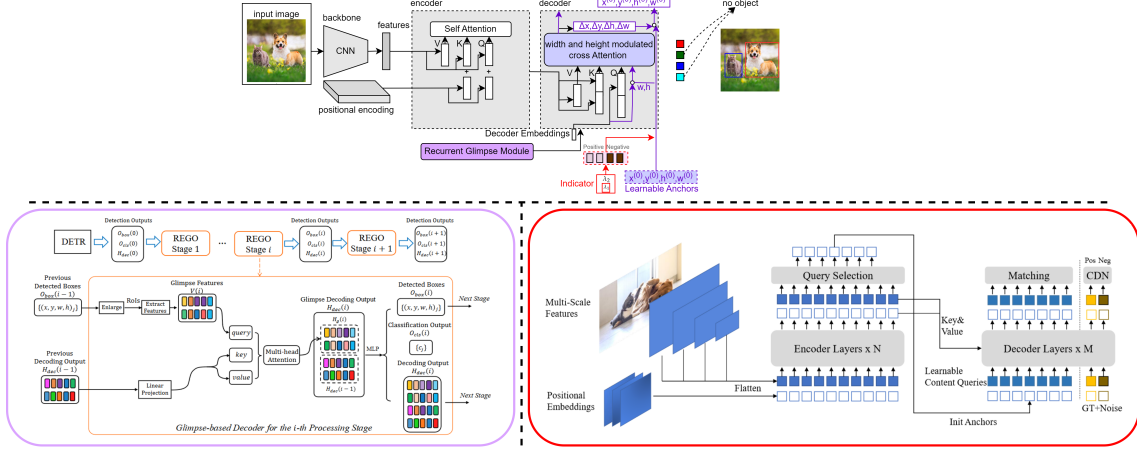


Fig. 9: The structure of the original DETR after the addition of REGO-DETR [26] and DINO [27]. Here, the top network is a simple DETR network, along with improvement indicated with small colored boxes. Larger boxes with corresponding colored borders are utilized to illustrate the internal mechanisms of these small colored boxes. The bottom left block indicates REGO-DETR and the bottom right box represents DINO (images from [26], [27]).

bilinear interpolation in the (x_i, y_i) space and then interpolates on the z-axis by gaussian weighting with weight for the i-th feature-map is as follows:

$$\tilde{w}_i = \frac{\exp(-(\tilde{z} - z_i^f)^2/\Gamma_z)}{\sum_i \exp(-(\tilde{z} - z_i^f)^2/\Gamma_z)} \quad (54)$$

where Γ_z is the softening coefficient to interpolate values over the z-axis ($\Gamma_z = 2$). This process makes the decoder detection learning easier by taking feature samples according the query.

AdaMixer Decoder: The decoder module in AdaMixer takes a content vector q_i and positional vector (x_i, y_i, z_i, r_i) as input object queries. The position aware multi-head self attention is applied between these queries as follows.

$$Attn(q_i, k_i, v_i) = \text{Softmax}(\frac{q_i k_i^T}{\sqrt{d}} + \alpha X).v_i \quad (55)$$

Where $X_{kl} = \log(|box_k \cap box_l|/|box_k| + \epsilon)$, $\epsilon = 10^{-7}$. The $X_{kl} = 0$ indicates the box_k is inside the box_l and $X_{kl} = 1$ represents no overlapping between box_k and box_l . This position vector is updated at every stage of decoder network. The AdaMixer decoder module takes a content vector and a positional vector as input object queries. For this, multi-scale features taken from the CNN backbone are converted into 3D feature space as the decoder should consider (x_i, y_i) space as well as adjustable in terms of scales of detected objects. It takes the sampled features from this feature space as input and applies the adaMixer mechanism to provide final predictions of input queries without using an encoder network to reduce the computational complexity of detection transformers.

4.20 REGO-DETR

REGO-DETR [26] proposes an ROI-based method for detection refinement to improve the attention mechanism in DETR. In Figure 9, the bottom left block denotes REGO-DETR. It contains two main modules: a multi-level recurrent mechanism and a glimpse-based decoder. In the multi-level recurrent mechanism, bounding boxes detected in the previous level are considered to get glimpse features, which are converted into refined attention using earlier attention in describing objects. The k-th processing level is as follows:

$$\begin{cases} O_{class}(k) = DF_{class}(H_{de}(k)) \\ O_{bbox}(k) = DF_{bbox}(H_{de}(k)) + O_{bbox}(k-1) \end{cases} \quad (56)$$

Where $O_{class} \in \mathbb{R}^{M_d \times M_c}$ and $O_{bbox} \in \mathbb{R}^{M_d \times 4}$. Here, M_d and M_c represents total number of predicted objects and classes, respectively. DF_{class} and DF_{bbox} are functions that convert the input features into desired outputs. $H_{de}(k)$ is the attention of this level after decoding as:

$$H_{de}(k) = [H_{gm}(k), H_{de}(k-1)] \quad (57)$$

where $H_{gm}(k)$ is the glimpse features according to $H_{de}(k-1)$ and previous levels. Then, these glimpse features are transformed using multi-head cross-attention into refined attention outputs according to previous attention outputs as:

$$H_{gm}(k) = Attn(V(k), H_{de}(k-1)), \quad (58)$$

For extracting the glimpse features $V(k)$, the following operation is performed:

$$V(k) = FE_{ext}(X, RI(O_{bbox}(k-1), \alpha(k))), \quad (59)$$

where FE_{ext} is the feature extraction function, $\alpha(k)$ is a scalar parameter and RI is the ROI computation. In this way, The Region-of-Interest (ROI) based refinement mod-

ules makes the training convergence of the detection transformer faster and provides better performance.

4.21 DINO

DN-DETR adds positive noise to the anchors taken as object queries to an input of the decoder and provides labels to only those anchors with ground-truth objects nearby. Following DAB-DETR and DN-DETR, DINO [27] solves this issue by proposing the Contrastive DeNoising (CDN) module that takes positional queries as anchor boxes and adds extra DN loss. In Figure 9, the bottom right block indicates DINO. This detector uses λ_1 and λ_2 hyperparameters where $\lambda_1 < \lambda_2$. The bounding box $b = (x_i, y_i, w_i, h_i)$ taken as input in the decoder, its corresponding generated anchor are denoted as $a = (x_i, y_i, w_i, h_i)$.

$$ATD(k) = \frac{1}{k} \sum \{ M_K(\{\|b_0 - a_0\|_1, \|b_1 - a_1\|_1, \dots, \|b_{N-1} - a_{N-1}\|_1\}, k) \} \quad (60)$$

Where $\| (b_i - a_i) \|$ is the distance between the anchor and bounding box and $M_K(x, k)$ is the function that provides the top K elements in x. The λ parameter is the threshold value for generating noise for anchors that are fed as input object queries to the decoder. It provides two types of anchor queries: positive with threshold value less than λ_1 and negative with noise threshold values greater than λ_1 and less than λ_2 . This way, the anchors with no ground-truth nearby are labelled as "no object". Thus, DINO makes the training convergence faster and improves performance for small objects.

5 DATASETS AND EVALUATION METRICS

To understand the effect of improvements in DETR on network size and performance, it is important to compare these methods. In this section, we present quantitative comparisons of improvements in DETR on popular benchmark MS COCO [30]. A mini val set of the COCO2014 is used for detection transformers evaluation. These results are evaluated using mean Average Precision (mAP) as the evaluation metric. The mAP is the mean of the Average Precision (AP) of each object category, where AP is the area under the precision-recall curve [210].

6 RESULTS AND DISCUSSION

Many advancements are proposed in DETR, such as backbone modification, Query design and attention refinement to improve performance and training convergence. Table 3 shows the performance comparison of all DETR-based detection transformers on the COCO minival set. We can observe that DETR performs well at 500 training epochs and has low AP on small objects. The modified versions improve performance and training convergence like DINO has mAP of 49.0% at 12 epochs and performs well on small objects. The backbone modifications, query design and attention refinement in DETR improved performance.

The quantitative analysis of DETR and its updated versions regarding training convergence and model size on the COCO minival set is performed. Part (a) of the Figure 10 shows the mAP of the detection transformers using a ResNet-50 backbone with training epochs. The original DETR, represented with a brown line, has low training convergence. It has an mAP value of 35.3% at 50 training epochs and 44.9 % at 500 training epochs. Here, DINO, represented with a red line, converges at low training epochs and gives the highest mAP on all epoch values. The attention mechanism in DETR involves computing pairwise attention scores between every pair of feature vectors, which can be computationally expensive, especially for large input images. Moreover, the self-attention mechanism in DETR relies on the use of fixed positional encodings to encode the spatial relationships between the different parts of the input image. This can slow down the training process and increase the time required to converge. In contrast, Deformable-DETR and DINO have some modifications that can help speed up the training process. For example, Deformable DETR introduces deformable attention layers, which can better capture spatial context information and improve the accuracy of object detection. Similarly, DINO uses a self-supervised learning approach to pre-train the network on unlabeled data before fine-tuning it for object detection. This pre-training can help the network learn more generalized features that can be useful for object detection, making the fine-tuning process faster and more effective.

Part (b) of Figure 10 compares all detection transformers regarding the model size. Here, YOLOS-DETR uses DeiT-small as the backbone instead of DeiT-Ti, but it also increases model size by 20x times. DINO and REGO-DETR have comparable mAP, but REGO-DETR is nearly double in model size than DINO. These networks use more complex architectures than the original DETR architecture, which increase the number of parameters in the model and the overall network size.

We also provide qualitative analysis of DETR and its updated versions on all-sized objects in Figure 11. For small objects, mAP for original DETR is 15.2% at 50 epochs, while DINO has an mAP value of 32% at 12 epochs. The self-attention mechanism in DINO allows it to interpolate features from neighboring pixels, which is particularly useful for small objects that may only occupy a few pixels in an image. This helps DINO to capture more precise and detailed information about small objects, which can lead to better performance compared to DETR. In contrast, DETR uses a multi-head self-attention mechanism, which can also capture context information but may not be as effective at interpolating features from neighboring pixels as DINO.

7 OPEN CHALLENGES & FUTURE DIRECTIONS

Detection Transformers have shown promising results on various object detection benchmarks, there are still some

TABLE 3: Performance comparison of all DETR-based detection transformers on COCO minival set. Here, networks labelled with DC5 take a dilated feature map. The IoU threshold values are set to 0.5 and 0.75 for AP calculation and also calculate AP for small(AP_s), medium(AP_m) and large(AP_l) objects. + represents bounding-box refinement and ++ denotes Deformable-DETR. ** indicates Efficient-DETR used 6-encoder layers and 1-decoder layer. S denotes Small, and B indicates Base. † represents distillation mechanism by Touvron et al. [211]. ‡ indicates model is Pre-trained on ImageNet-21k. All models use 300 queries, while DETR uses 100 object queries to the input of decoder network. The models with superscript * use 3 pattern embeddings. The three best results are represented in red, blue, and green, respectively.

Methods	Backbone	Publications	Epoch	GFLOPs	Parameters (M)	AP	AP ⁵⁰	AP ⁷⁵	AP _S	AP _M	AP _L
Faster R-CNN [194]	DC5-ResNet-50	CVPR 2015	109	320	166	41.1	61.4	44.3	22.9	45.9	55.0
	ResNet-50-FPN		109	180	42	42.0	62.1	45.5	26.6	45.4	53.4
	ResNet-101-FPN		109	246	60	44.0	63.9	47.8	27.2	48.1	56.0
DETR [7]	DC5-ResNet-50	ECCV 2020	50	187	41	35.3	55.7	36.8	15.2	37.5	53.6
	DC5-ResNet-50		500	187	41	43.3	63.1	45.9	22.5	47.3	61.1
	DC5-ResNet-101		500	253	60	44.9	64.7	47.7	23.7	49.5	62.3
Deformable-DETR [9]	ResNet-50	ICLR 2021	50	173	40	43.8	62.6	47.7	26.4	47.1	58.0
	ResNet-50+		50	173	40	45.4	64.7	49.0	26.8	48.3	61.7
	ResNet-50++		50	173	40	46.2	65.2	50.0	28.8	49.2	61.7
UP-DETR [10]	ResNet-50	CVPR 2021	150	86	41	40.5	60.8	42.6	19.0	44.4	60.0
	ResNet-50		300	86	41	42.8	63.0	45.3	20.8	47.1	61.7
Efficient-DETR [11]	ResNet-50	arXiv 2021	36	159	32	44.2	62.2	48.0	28.4	47.5	56.6
	ResNet-101		36	239	51	45.2	63.7	48.8	28.8	49.1	59.0
	ResNet-101 **		36	289	54	45.7	64.1	49.5	28.2	49.1	60.2
SMCA-DETR [12]	ResNet-50	ICCV 2021	50	152	40	43.7	63.6	47.2	24.2	47.0	60.4
	ResNet-50		108	152	40	45.6	65.5	49.1	25.9	49.3	62.6
	ResNet-101		50	218	58	44.4	65.2	48.0	24.3	48.5	61.0
TSP-DETR [28]	FCOS-ResNet-50	ICCV 2021	36	189	51.5	43.1	62.3	47.0	26.6	46.8	55.9
	RCNN-ResNet-50		36	188	63.6	43.8	63.3	48.3	28.6	46.9	55.7
Conditional-DETR [14]	DC5-ResNet-50	ICCV 2021	50	195	44	43.8	64.4	46.7	24.0	47.6	60.7
	DC5-ResNet-101		50	262	63	45.0	65.5	48.4	26.1	48.9	62.8
WB-DETR [15]	-	ICCV 2021	500	98	24	41.8	63.2	44.8	19.4	45.1	62.4
PnP-DETR [16]	DC5-ResNet-50	ICCV 2021	500	145	41	43.1	63.4	45.3	22.7	46.5	61.1
Dynamc-DETR [17]	ResNet-50	ICCV 2021	12	-	58	42.9	61.0	46.3	24.6	44.9	54.4
YOLOS-DETR [18]	DeiT-S [211] †	NeurIPS 2021	150	194	31	36.1	56.5	37.1	15.3	38.5	56.2
	DeiT-B [211] †		150	538	127	42.0	62.2	44.5	19.5	45.3	62.1
Anchor-DETR [19]	DC5-ResNet-50 *	AAAI 2022	50	151	39	44.2	64.7	47.5	24.7	48.2	60.6
	DC5-ResNet-101 *		50	237	58	45.1	65.7	48.8	25.8	49.4	61.6
Sparse-DETR [20]	ResNet-50- ρ -0.5	ICLR 2022	50	136	41	46.3	66.0	50.1	29.0	49.5	60.8
	Swin-T- ρ -0.5 [212]		50	144	41	49.3	69.5	53.3	32.0	52.7	64.9
D ² ETR [21]	PVT2	arXiv 2022	50	82	35	43.2	62.9	46.2	22.0	48.5	62.4
	Def D ² ETR [21]		50	93	40	50.0	67.9	54.1	31.7	53.4	66.7
FP-DETR-S [22]	-	ICLR 2022	50	102	24	42.5	62.6	45.9	25.3	45.5	56.9
	FP-DETR-B [22]		50	121	36	43.3	63.9	47.7	27.5	46.1	57.0
	FP-DETR-B ‡ [22]		50	121	36	43.7	64.1	47.8	26.5	46.7	58.2
CF-DETR [23]	ResNet-50	AAAI 2022	36	-	-	47.8	66.5	52.4	31.2	50.6	62.8
	ResNet-101		36	-	-	49.0	68.1	53.4	31.4	52.2	64.3
DAB-DETR [29]	DC5-ResNet-50 *	ICLR 2022	50	216	44	45.7	66.2	49.0	26.1	49.4	63.1
	DC5-ResNet-101 *		50	296	63	46.6	67.0	50.2	28.1	50.5	64.1
DN-DETR [24]	ResNet-50	CVPR 2022	50	94	44	44.1	64.4	46.7	22.9	48.0	63.4
	DC5-ResNet-50		50	202	44	46.3	66.4	49.7	26.7	50.0	64.3
	ResNet-101		50	174	63	45.2	65.5	48.3	24.1	49.1	65.1
	DC5-ResNet-101		50	282	63	47.3	67.5	50.8	28.6	51.5	65.0
AdaMixer [25]	ResNet-50	CVPR 2022	36	132	139	47.0	66.0	51.1	30.1	50.2	61.8
	ResNeXt-101-DCN		36	214	160	49.5	68.9	53.9	31.3	52.3	66.3
	Swin-s [212]		36	234	164	51.3	71.2	55.7	34.2	54.6	67.3
REGO [26]	ResNet-50++	CVPR 2022	50	190	54	47.6	66.8	51.6	29.6	50.6	62.3
	ResNet-101++		50	257	73	48.5	67.0	52.4	29.5	52.0	64.4
	ReNeXt-101++		50	434	119	49.1	67.5	53.1	30.0	52.6	65.0
DINO [27]	ReNet-50-4scale *	arXiv 2022	12	279	47	49.0	66.6	53.5	32.0	52.3	63.0
	ResNet-50-5scale *		12	860	47	49.4	66.9	53.8	32.3	52.5	63.9
	ReNet-50-5scale *		24	860	47	51.3	69.1	56.0	34.5	54.2	65.8
	ResNet-50-5scale *		36	860	47	51.2	69.0	55.8	35.0	54.3	65.3

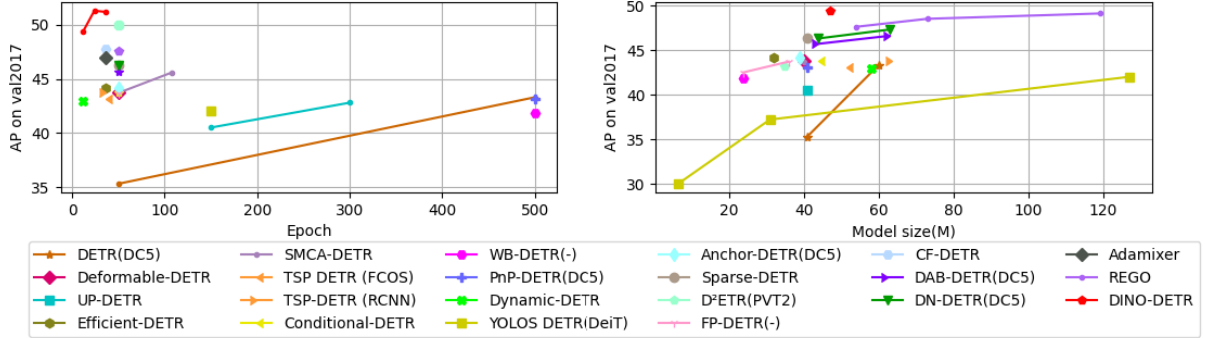


Fig. 10: Comparison of all DETR-based detection transformers on COCO minival set. (a) Performance comparison of detection transformers using a ResNet-50 [66] backbone w.r.t. training epochs. Networks that are labelled with DC5 take a dilated feature-map. (b) Performance comparison of detection transformers w.r.t. model size (parameters in million).

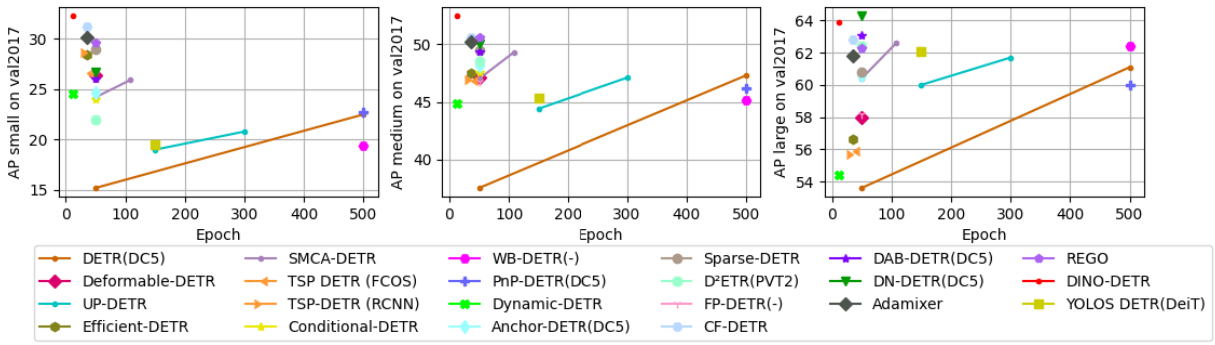


Fig. 11: Comparison of DETR-based detection transformers on COCO minival set using a ResNet-50 backbone. (a) Performance comparison of detection transformers on small objects. (b) Performance comparison of detection transformers on medium objects. (c) Performance comparison of detection transformers on large objects.

open challenges and future directions for improving it. Table 4 provides advantages and limitations of all proposed improved versions of DETR. Here are some of the open challenges and future directions for improvements in DETR:

Scaling to Large Datasets: DINO, an improved version of DETR, has shown impressive results on small and medium-sized datasets, but its performance drops when scaled to large datasets. Future work should explore ways to scale detection transformers to large datasets while maintaining their performance.

Improving Sample Efficiency: Detection Transformers require a large amount of training data to learn effective representations. Future work should investigate ways to improve sample efficiency, such as incorporating domain-specific knowledge or using active learning techniques.

Handling Long-Tailed Distributions: Detection Transformers struggle with long-tailed distributions, where some classes have much fewer instances than others. Future work should explore ways to address this class imbalance, such

as using re-sampling techniques.

Incorporating local & global Information: DETR focuses on global information, while DINO focuses on learning local representations from images. However, DETR and its improved version do not explicitly model local & global Information of different parts of an image. Future work should explore incorporating both information into the model.

Overall, there is still much room for improvement in detection transformer, and addressing these open challenges and future directions will likely lead to even more impressive results.

8 CONCLUSION

Detection transformers have provided efficient and precise object detection networks and delivered insights into the operation of deep neural networks. This review gives a detailed overview of the Detection Transformers. Specifically, it focuses on the latest advancements in DETR to improve performance and training convergence. The attention

TABLE 4: Overview of Advantages and limitations of Detection Transformers.

Methods	Publications	Advantages	Limitations
DETR [7]	ECCV 2020	Removes the need for hand-designed components like NMS or anchor generation.	Low performance on small objects and slow training convergence.
Deformable-DETR [9]	ICLR 2021	Deformable attention network, which makes training convergence faster.	Number of encoder tokens increases by 20 times compared to DETR.
UP-DETR [10]	CVPR 2021	Pre-training for Multi-tasks learning and Multi-queries localization.	Pre-training for patch localization, CNN and transformers pre-training needs to integrate.
Efficient-DETR [11]	arXiv 2021	Reduces decoder layers by employing dense and sparse set based network	Increase in GFLOPs twice compared to original DETR.
SMCA-DETR [12]	ICCV 2021	Regression-aware mechanism to increase convergence speed	Low performance in detecting small objects.
TSP-DETR [28]	ICCV 2021	Deals with issues of Hungarian loss and the cross-attention mechanism of Transformer.	Uses proposals in TSP-FCOS and feature points in TSP-RCNN as in CNN-based detectors.
Conditional-DETR [14]	ICCV 2021	Conditional queries remove dependency on content embeddings and ease the training.	Performs better than DETR and deformable-DETR for stronger backbones.
WB-DETR [15]	ICCV 2021	Pure transformer network without backbone.	Low performance on small objects.
PnP-DETR [16]	ICCV 2021	Sampling module provides foreground and a small quantity of background features.	Breaks 2d spatial structure by taking foreground tokens and reducing background tokens.
Dynamic-DETR [17]	ICCV 2021	Dynamic attention provides small feature resolution and improves training convergence.	Still dependent on CNN networks as convolution-based encoder and an ROI-based decoder.
YOLOS-DETR [18]	NeurIPS 2021	Convert ViT pre-trained on ImageNet-1k dataset into Object detector.	Pre-trained ViT still needs improvements as it requires long training epochs.
Anchor-DETR [19]	AAAI 2022	Object queries as anchor points that predict multiple objects at one position.	Consider queries as 2D anchor points which ignore object scale.
Spare-DETR [20]	ICLR 2022	Improve performance by updating tokens referenced by the decoder.	Performance is strongly dependent on the backbone specifically for large objects.
D^2 ETR [21]	arXiv 2022	Decoder-only transformer network to reduce computational cost.	Decreases computation complexity significantly but has low performance on small objects.
FP-DETR [22]	ICLR 2022	Pre-Training of encoder-only transformer.	Low performance on large objects.
CF-DETR [23]	AAAI 2022	Refine coarse features to improve localization accuracy of small objects.	Addition of three new modules increase network size.
DAB-DETR [29]	ICLR 2022	Anchor-boxes as queries, attention for different scale objects.	Positional prior for only foreground objects.
DN-DETR [24]	CVPR 2022	Denoising training for positional-prior for foreground and background regions.	Denoising training by adding positive noise to object queries ignoring background regions.
AdaMixer [25]	CVPR 2022	Faster Convergence, Improves the adaptability of query-based decoding mechanism.	Large number of parameters.
REGO [26]	CVPR 2022	Attention mechanism gradually focus on foreground regions more accurately.	Multi-stage RoI-based attention modeling increases number of parameters.
DINO [27]	arXiv 2022	impressive results on small and medium-sized datasets	Performance drops for large size objects

module of the detection transformer in the encoder-decoder network is modified to improve training convergence, and object queries as input to the decoder are updated to improve performance for small objects. We provide the latest improvements in detection transformers, including backbone modification, query design and attention refinement. We also compare the advantages and limitations of detection transformers in terms of performance and architectural design. With its focus on object detection tasks, this review provides a unique view of the recent advancement in DETR. We hope this study will increase the researcher's interest in solving existing challenges towards applying transformers models in the object detection domain.

ACKNOWLEDGMENTS

The work has been partially funded by the European project INFINITY under Grant Agreement ID 883293.

REFERENCES

- [1] S. Ren, K. He, R. B. Girshick, and J. Sun, "Faster R-CNN: towards real-time object detection with region proposal networks," *CoRR*, vol. abs/1506.01497, 2015. [Online]. Available: <http://arxiv.org/abs/1506.01497>
- [2] R. B. Girshick, "Fast R-CNN," *CoRR*, vol. abs/1504.08083, 2015. [Online]. Available: <http://arxiv.org/abs/1504.08083>
- [3] J. Redmon and A. Farhadi, "Yolov3: An incremental improvement," *CoRR*, vol. abs/1804.02767, 2018. [Online]. Available: <http://arxiv.org/abs/1804.02767>
- [4] T. Lin, P. Goyal, R. B. Girshick, K. He, and P. Dollár, "Focal loss for dense object detection," *CoRR*, vol. abs/1708.02002, 2017. [Online]. Available: <http://arxiv.org/abs/1708.02002>
- [5] A. Dosovitskiy, L. Beyer, A. Kolesnikov, D. Weissenborn, X. Zhai, T. Unterthiner, M. Dehghani, M. Minderer, G. Heigold, S. Gelly, J. Uszkoreit, and N. Houlsby, "An image is worth 16x16 words: Transformers for image recognition at scale," *CoRR*, vol. abs/2010.11929, 2020. [Online]. Available: <https://arxiv.org/abs/2010.11929>
- [6] A. Vaswani, N. Shazeer, N. Parmar, J. Uszkoreit, L. Jones, A. N. Gomez, L. u. Kaiser, and I. Polosukhin, "Attention is all you need," in *Advances in Neural Information Processing Systems*, I. Guyon, U. V. Luxburg, S. Bengio, H. Wallach, R. Fergus, S. Vishwanathan, and R. Garnett, Eds., vol. 30. Curran Associates, Inc., 2017. [Online]. Available: <https://proceedings.neurips.cc/paper/2017/file/3f5ee243547dee91fb0d053c1c4a845aa-Paper.pdf>
- [7] N. Carion, F. Massa, G. Synnaeve, N. Usunier, A. Kirillov, and S. Zagoruyko, "End-to-end object detection with transformers," in *European conference on computer vision*. Springer, 2020, pp. 213–229.
- [8] R. B. Girshick, J. Donahue, T. Darrell, and J. Malik, "Rich feature hierarchies for accurate object detection and semantic segmentation," *CoRR*, vol. abs/1311.2524, 2013. [Online]. Available: <http://arxiv.org/abs/1311.2524>
- [9] X. Zhu, W. Su, L. Lu, B. Li, X. Wang, and J. Dai, "Deformable DETR: deformable transformers for end-to-end object detection," *CoRR*, vol. abs/2010.04159, 2020. [Online]. Available: <https://arxiv.org/abs/2010.04159>
- [10] Z. Dai, B. Cai, Y. Lin, and J. Chen, "UP-DETR: unsupervised pre-training for object detection with transformers," *CoRR*, vol.

abs/2011.09094, 2020. [Online]. Available: <https://arxiv.org/abs/2011.09094>

[11] Z. Yao, J. Ai, B. Li, and C. Zhang, "Efficient DETR: improving end-to-end object detector with dense prior," *CoRR*, vol. abs/2104.01318, 2021. [Online]. Available: <https://arxiv.org/abs/2104.01318>

[12] P. Gao, M. Zheng, X. Wang, J. Dai, and H. Li, "Fast convergence of DETR with spatially modulated co-attention," *CoRR*, vol. abs/2101.07448, 2021. [Online]. Available: <https://arxiv.org/abs/2101.07448>

[13] Z. Sun, S. Cao, Y. Yang, and K. Kitani, "Rethinking transformer-based set prediction for object detection," *CoRR*, vol. abs/2011.10881, 2020. [Online]. Available: <https://arxiv.org/abs/2011.10881>

[14] D. Meng, X. Chen, Z. Fan, G. Zeng, H. Li, Y. Yuan, L. Sun, and J. Wang, "Conditional DETR for fast training convergence," *CoRR*, vol. abs/2108.06152, 2021. [Online]. Available: <https://arxiv.org/abs/2108.06152>

[15] F. Liu, H. Wei, W. Zhao, G. Li, J. Peng, and Z. Li, "Wbdetr: Transformer-based detector without backbone," in *2021 IEEE/CVF International Conference on Computer Vision (ICCV)*, 2021, pp. 2959–2967.

[16] T. Wang, L. Yuan, Y. Chen, J. Feng, and S. Yan, "Pnpdetr: Towards efficient visual analysis with transformers," *CoRR*, vol. abs/2109.07036, 2021. [Online]. Available: <https://arxiv.org/abs/2109.07036>

[17] X. Dai, Y. Chen, J. Yang, P. Zhang, L. Yuan, and L. Zhang, "Dynamic detr: End-to-end object detection with dynamic attention," in *2021 IEEE/CVF International Conference on Computer Vision (ICCV)*, pp. 2968–2977, 2021.

[18] Y. Fang, B. Liao, X. Wang, J. Fang, J. Qi, R. Wu, J. Niu, and W. Liu, "You only look at one sequence: Rethinking transformer in vision through object detection," *CoRR*, vol. abs/2106.00666, 2021. [Online]. Available: <https://arxiv.org/abs/2106.00666>

[19] Y. Wang, X. Zhang, T. Yang, and J. Sun, "Anchor detr: Query design for transformer-based detector," in *AAAI Conference on Artificial Intelligence*, 2022.

[20] B. Roh, J. Shin, W. Shin, and S. Kim, "Sparse DETR: efficient end-to-end object detection with learnable sparsity," *CoRR*, vol. abs/2111.14330, 2021. [Online]. Available: <https://arxiv.org/abs/2111.14330>

[21] J. Lin, X. Mao, Y. Chen, L. Xu, Y. He, and H. Xue, "d²etr: Decoder-only detr with computationally efficient cross-scale attention," 2022. [Online]. Available: <https://arxiv.org/abs/2203.00860>

[22] W. Wang, Y. Cao, J. Zhang, and D. Tao, "FP-DETR: Detection transformer advanced by fully pre-training," in *International Conference on Learning Representations*, 2022. [Online]. Available: <https://openreview.net/forum?id=yjMQuLLcGWK>

[23] X. Cao, P. Yuan, B. Feng, and K. Niu, "Cf-detr: Coarse-to-fine transformers for end-to-end object detection," 2022.

[24] F. Li, H. Zhang, S. Liu, J. Guo, L. M. Ni, and L. Zhang, "Dn-detr: Accelerate detr training by introducing query denoising," in *Proceedings of the IEEE/CVF Conference on Computer Vision and Pattern Recognition*, 2022, pp. 13619–13627.

[25] Z. Gao, L. Wang, B. Han, and S. Guo, "Adamixer: A fast-converging query-based object detector," 2022. [Online]. Available: <https://arxiv.org/abs/2203.16507>

[26] Z. Chen, J. Zhang, and D. Tao, "Recurrent glimpse-based decoder for detection with transformer," *CoRR*, vol. abs/2112.04632, 2021. [Online]. Available: <https://arxiv.org/abs/2112.04632>

[27] H. Zhang, F. Li, S. Liu, L. Zhang, H. Su, J. Zhu, L. M. Ni, and H.-Y. Shum, "Dino: Detr with improved denoising anchor boxes for end-to-end object detection," 2022. [Online]. Available: <https://arxiv.org/abs/2203.03605>

[28] Z. Sun, S. Cao, Y. Yang, and K. Kitani, "Rethinking transformer-based set prediction for object detection," *CoRR*, vol. abs/2011.10881, 2020. [Online]. Available: <https://arxiv.org/abs/2011.10881>

[29] S. Liu, F. Li, H. Zhang, X. Yang, X. Qi, H. Su, J. Zhu, and L. Zhang, "DAB-DETR: dynamic anchor boxes are better queries for DETR," *CoRR*, vol. abs/2201.12329, 2022. [Online]. Available: <https://arxiv.org/abs/2201.12329>

[30] T. Lin, M. Maire, S. J. Belongie, L. D. Bourdev, R. B. Girshick, J. Hays, P. Perona, D. Ramanan, P. Dollár, and C. L. Zitnick, "Microsoft COCO: common objects in context," *CoRR*, vol. abs/1405.0312, 2014. [Online]. Available: <http://arxiv.org/abs/1405.0312>

[31] J. Han, D. Zhang, G. Cheng, N. Liu, and D. Xu, "Advanced deep-learning techniques for salient and category-specific object detection: A survey," *IEEE Signal Processing Magazine*, vol. 35, no. 1, pp. 84–100, 2018.

[32] Z. Zou, Z. Shi, Y. Guo, and J. Ye, "Object detection in 20 years: A survey," *CoRR*, vol. abs/1905.05055, 2019. [Online]. Available: <http://arxiv.org/abs/1905.05055>

[33] L. Liu, W. Ouyang, X. Wang, P. W. Fieguth, J. Chen, X. Liu, and M. Pietikäinen, "Deep learning for generic object detection: A survey," *CoRR*, vol. abs/1809.02165, 2018. [Online]. Available: <http://arxiv.org/abs/1809.02165>

[34] I. Ülkü and E. Akagündüz, "A survey on deep learning-based architectures for semantic segmentation on 2d images," *CoRR*, vol. abs/1912.10230, 2019. [Online]. Available: <http://arxiv.org/abs/1912.10230>

[35] S. S. A. Zaidi, M. S. Ansari, A. Aslam, N. Kanwal, M. N. Asghar, and B. Lee, "A survey of modern deep learning based object detection models," *CoRR*, vol. abs/2104.11892, 2021. [Online]. Available: <https://arxiv.org/abs/2104.11892>

[36] E. Arkin, N. Yadikar, Y. Muhtar, and K. Ubul, "A survey of object detection based on cnn and transformer," in *2021 IEEE 2nd International Conference on Pattern Recognition and Machine Learning (PRML)*, 2021, pp. 99–108.

[37] S. Khan, M. Naseer, M. Hayat, S. W. Zamir, F. S. Khan, and M. Shah, "Transformers in vision: A survey," *ACM Comput. Surv.*, vol. 54, no. 10s, sep 2022. [Online]. Available: <https://doi.org/10.1145/3505244>

[38] E. Arkin, N. Yadikar, X. Xu, A. Aysa, and K. Ubul, "A survey: object detection methods from cnn to transformer," *Multimedia Tools and Applications*, pp. 1–31, 2022.

[39] K. Han, Y. Wang, H. Chen, X. Chen, J. Guo, Z. Liu, Y. Tang, A. Xiao, C. Xu, Y. Xu, Z. Yang, Y. Zhang, and D. Tao, "A survey on vision transformer," *IEEE Transactions on Pattern Analysis and Machine Intelligence*, vol. 45, no. 1, pp. 87–110, 2023.

[40] J. Gu, Z. Wang, J. Kuen, L. Ma, A. Shahroudy, B. Shuai, T. Liu, X. Wang, and G. Wang, "Recent advances in convolutional neural networks," *CoRR*, vol. abs/1512.07108, 2015. [Online]. Available: <http://arxiv.org/abs/1512.07108>

[41] A. Borji, M. Cheng, H. Jiang, and J. Li, "Salient object detection: A survey," *CoRR*, vol. abs/1411.5878, 2014. [Online]. Available: <http://arxiv.org/abs/1411.5878>

[42] G. Chen, H. Wang, K. Chen, Z. Li, Z. Song, Y. Liu, W. Chen, and A. Knoll, "A survey of the four pillars for small object detection: Multiscale representation, contextual information, super-resolution, and region proposal," *IEEE Transactions on Systems, Man, and Cybernetics: Systems*, vol. 52, no. 2, pp. 936–953, 2022.

[43] S. Agarwal, J. O. du Terrail, and F. Jurie, "Recent advances in object detection in the age of deep convolutional neural networks," *CoRR*, vol. abs/1809.03193, 2018. [Online]. Available: <http://arxiv.org/abs/1809.03193>

[44] M.-H. Yang, D. Kriegman, and N. Ahuja, "Detecting faces in images: a survey," *IEEE Transactions on Pattern Analysis and Machine Intelligence*, vol. 24, no. 1, pp. 34–58, 2002.

[45] B. Zhao, J. Feng, X. Wu, and S. Yan, "A survey on deep learning-based fine-grained object classification and semantic segmentation," *International Journal of Automation and Computing*, vol. 14, no. 2, pp. 119–135, 2017.

[46] T. Goswami, Z. Barad, P. Desai, and P. Nikita, "Text detection and recognition in images: A survey," *arXiv preprint arXiv:1803.07278*, 2018.

[47] S. Chaudhari, G. Polatkan, R. Ramanath, and V. Mithal, "An attentive survey of attention models," *CoRR*, vol. abs/1904.02874, 2019. [Online]. Available: <http://arxiv.org/abs/1904.02874>

[48] M. Enzweiler and D. M. Gavrila, "Monocular pedestrian detection: Survey and experiments," *IEEE Transactions on Pattern Analysis and Machine Intelligence*, vol. 31, no. 12, pp. 2179–2195, 2009.

[49] G. Cheng and J. Han, "A survey on object detection in optical remote sensing images," *CoRR*, vol. abs/1603.06201, 2016. [Online]. Available: <http://arxiv.org/abs/1603.06201>

[50] L. W. Sommer, T. Schuchert, and J. Beyerer, "Fast deep vehicle detection in aerial images," in *2017 IEEE Winter Conference on Applications of Computer Vision (WACV)*, 2017, pp. 311–319.

[51] P. Zhang, X. Niu, Y. Dou, and F. Xia, "Airport detection on optical satellite images using deep convolutional neural networks," *IEEE Geoscience and Remote Sensing Letters*, vol. 14, no. 8, pp. 1183–1187, 2017.

[52] M. Bach, D. Stumper, and K. Dietmayer, "Deep convolutional traffic light recognition for automated driving," in *2018 21st International Conference on Intelligent Transportation Systems (ITSC)*, 2018, pp. 851–858.

[53] A. de la Escalera, L. Moreno, M. Salichs, and J. Armingol, "Road traffic sign detection and classification," *IEEE Transactions on Industrial Electronics*, vol. 44, no. 6, pp. 848–859, 1997.

[54] T. Shehzadi, K. A. Hashmi, A. Pagani, M. Liwicki, D. Stricker, and M. Z. Afzal, "Mask-aware semi-supervised object detection in floor plans," *Applied Sciences*, vol. 12, no. 19, 2022. [Online]. Available: <https://www.mdpi.com/2076-3417/12/19/9398>

[55] B. Hariharan, P. Arbelaez, R. B. Girshick, and J. Malik, "Simultaneous detection and segmentation," *CoRR*, vol. abs/1407.1808, 2014. [Online]. Available: <http://arxiv.org/abs/1407.1808>

[56] B. Hariharan, P. A. Arbelaez, R. B. Girshick, and J. Malik, "Hypercolumns for object segmentation and fine-grained localization," *CoRR*, vol. abs/1411.5752, 2014. [Online]. Available: <http://arxiv.org/abs/1411.5752>

[57] J. Dai, K. He, and J. Sun, "Instance-aware semantic segmentation via multi-task network cascades," *CoRR*, vol. abs/1512.04412, 2015. [Online]. Available: <http://arxiv.org/abs/1512.04412>

[58] A. Karpathy and L. Fei-Fei, "Deep visual-semantic alignments for generating image descriptions," *CoRR*, vol. abs/1412.2306, 2014. [Online]. Available: <http://arxiv.org/abs/1412.2306>

[59] K. Xu, J. Ba, R. Kiros, K. Cho, A. C. Courville, R. Salakhutdinov, R. S. Zemel, and Y. Bengio, "Show, attend and tell: Neural image caption generation with visual attention," *CoRR*, vol. abs/1502.03044, 2015. [Online]. Available: <http://arxiv.org/abs/1502.03044>

[60] Q. Wu, C. Shen, A. van den Hengel, P. Wang, and A. R. Dick, "Image captioning and visual question answering based on attributes and their related external knowledge," *CoRR*, vol. abs/1603.02814, 2016. [Online]. Available: <http://arxiv.org/abs/1603.02814>

[61] S. Bai and S. An, "A survey on automatic image caption generation," *Neurocomputing*, vol. 311, pp. 291–304, 2018.

[62] K. Kang, H. Li, J. Yan, X. Zeng, B. Yang, T. Xiao, C. Zhang, Z. Wang, R. Wang, X. Wang, and W. Ouyang, "T-CNN: tubelets with convolutional neural networks for object detection from videos," *CoRR*, vol. abs/1604.02532, 2016. [Online]. Available: <http://arxiv.org/abs/1604.02532>

[63] L. Jiao, F. Zhang, F. Liu, S. Yang, L. Li, Z. Feng, and R. Qu, "A survey of deep learning-based object detection," *CoRR*, vol. abs/1907.09408, 2019. [Online]. Available: <http://arxiv.org/abs/1907.09408>

[64] M. Everingham, L. V. Gool, C. K. I. Williams, J. Winn, and A. Zisserman, "The pascal visual object classes (voc) challenge," *International Journal of Computer Vision*, vol. 88, pp. 303–308, September 2009, printed version publication date: June 2010. [On-

line]. Available: <https://www.microsoft.com/en-us/research/publication/the-pascal-visual-object-classes-voc-challenge/>

[65] T.-Y. Lin, P. Dollár, R. Girshick, K. He, B. Hariharan, and S. Belongie, "Feature pyramid networks for object detection," in *2017 IEEE Conference on Computer Vision and Pattern Recognition (CVPR)*, 2017, pp. 936–944.

[66] K. He, X. Zhang, S. Ren, and J. Sun, "Deep residual learning for image recognition," *CoRR*, vol. abs/1512.03385, 2015. [Online]. Available: <http://arxiv.org/abs/1512.03385>

[67] A. Krizhevsky, I. Sutskever, and G. E. Hinton, "Imagenet classification with deep convolutional neural networks," in *Advances in Neural Information Processing Systems*, F. Pereira, C. Burges, L. Bottou, and K. Weinberger, Eds., vol. 25. Curran Associates, Inc., 2012. [Online]. Available: <https://proceedings.neurips.cc/paper/2012/file/c399862d3b9d6b76c8436e924a68c45b-Paper.pdf>

[68] A. Bar, X. Wang, V. Kantorov, C. J. Reed, R. Herzig, G. Chechik, A. Rohrbach, T. Darrell, and A. Globerson, "Detreg: Unsupervised pretraining with region priors for object detection," *CoRR*, vol. abs/2106.04550, 2021. [Online]. Available: <https://arxiv.org/abs/2106.04550>

[69] P. Bateni, J. Barber, J. van de Meent, and F. Wood, "Improving few-shot visual classification with unlabelled examples," *CoRR*, vol. abs/2006.12245, 2020. [Online]. Available: <https://arxiv.org/abs/2006.12245>

[70] X. Wang, X. Yang, S. Zhang, Y. Li, L. Feng, S. Fang, C. Lyu, K. Chen, and W. Zhang, "Consistent targets provide better supervision in semi-supervised object detection," 2022. [Online]. Available: <https://arxiv.org/abs/2209.01589>

[71] Y. Li, D. Huang, D. Qin, L. Wang, and B. Gong, "Improving object detection with selective self-supervised self-training," *CoRR*, vol. abs/2007.09162, 2020. [Online]. Available: <https://arxiv.org/abs/2007.09162>

[72] M. Caron, H. Touvron, I. Misra, H. Jégou, J. Mairal, P. Bojanowski, and A. Joulin, "Emerging properties in self-supervised vision transformers," *CoRR*, vol. abs/2104.14294, 2021. [Online]. Available: <https://arxiv.org/abs/2104.14294>

[73] C. Li, J. Yang, P. Zhang, M. Gao, B. Xiao, X. Dai, L. Yuan, and J. Gao, "Efficient self-supervised vision transformers for representation learning," *CoRR*, vol. abs/2106.09785, 2021. [Online]. Available: <https://arxiv.org/abs/2106.09785>

[74] J. Redmon and A. Farhadi, "Yolov3: An incremental improvement," *CoRR*, vol. abs/1804.02767, 2018. [Online]. Available: <http://arxiv.org/abs/1804.02767>

[75] W. Liu, D. Anguelov, D. Erhan, C. Szegedy, S. E. Reed, C. Fu, and A. C. Berg, "SSD: single shot multibox detector," *CoRR*, vol. abs/1512.02325, 2015. [Online]. Available: <http://arxiv.org/abs/1512.02325>

[76] J. Redmon, S. K. Divvala, R. B. Girshick, and A. Farhadi, "You only look once: Unified, real-time object detection," *CoRR*, vol. abs/1506.02640, 2015. [Online]. Available: <http://arxiv.org/abs/1506.02640>

[77] J. Redmon and A. Farhadi, "YOLO9000: better, faster, stronger," *CoRR*, vol. abs/1612.08242, 2016. [Online]. Available: <http://arxiv.org/abs/1612.08242>

[78] A. Bochkovskiy, C. Wang, and H. M. Liao, "Yolov4: Optimal speed and accuracy of object detection," *CoRR*, vol. abs/2004.10934, 2020. [Online]. Available: <https://arxiv.org/abs/2004.10934>

[79] X. Zhou, D. Wang, and P. Krähenbühl, "Objects as points," *CoRR*, vol. abs/1904.07850, 2019. [Online]. Available: <http://arxiv.org/abs/1904.07850>

[80] C. Fu, W. Liu, A. Ranga, A. Tyagi, and A. C. Berg, "DSSD : Deconvolutional single shot detector," *CoRR*, vol. abs/1701.06659, 2017. [Online]. Available: <http://arxiv.org/abs/1701.06659>

[81] J. Jeong, H. Park, and N. Kwak, "Enhancement of SSD by concatenating feature maps for object detection," *CoRR*, vol.

abs/1705.09587, 2017. [Online]. Available: <http://arxiv.org/abs/1705.09587>

[82] S. Zhang, L. Wen, X. Bian, Z. Lei, and S. Z. Li, "Single-shot refinement neural network for object detection," *CoRR*, vol. abs/1711.06897, 2017. [Online]. Available: <http://arxiv.org/abs/1711.06897>

[83] H. Law and J. Deng, "Cornernet: Detecting objects as paired keypoints," *CoRR*, vol. abs/1808.01244, 2018. [Online]. Available: <http://arxiv.org/abs/1808.01244>

[84] K. He, X. Zhang, S. Ren, and J. Sun, "Spatial pyramid pooling in deep convolutional networks for visual recognition," *CoRR*, vol. abs/1406.4729, 2014. [Online]. Available: <http://arxiv.org/abs/1406.4729>

[85] J. Dai, Y. Li, K. He, and J. Sun, "R-FCN: object detection via region-based fully convolutional networks," *CoRR*, vol. abs/1605.06409, 2016. [Online]. Available: <http://arxiv.org/abs/1605.06409>

[86] K. He, G. Gkioxari, P. Dollár, and R. Girshick, "Mask r-cnn," in *2017 IEEE International Conference on Computer Vision (ICCV)*, 2017, pp. 2980–2988.

[87] S. Qiao, L. Chen, and A. L. Yuille, "Detectors: Detecting objects with recursive feature pyramid and switchable atrous convolution," *CoRR*, vol. abs/2006.02334, 2020. [Online]. Available: <https://arxiv.org/abs/2006.02334>

[88] K. Chen, J. Pang, J. Wang, Y. Xiong, X. Li, S. Sun, W. Feng, Z. Liu, J. Shi, W. Ouyang, C. C. Loy, and D. Lin, "Hybrid task cascade for instance segmentation," *CoRR*, vol. abs/1901.07518, 2019. [Online]. Available: <http://arxiv.org/abs/1901.07518>

[89] Z. Cai and N. Vasconcelos, "Cascade R-CNN: delving into high quality object detection," *CoRR*, vol. abs/1712.00726, 2017. [Online]. Available: <http://arxiv.org/abs/1712.00726>

[90] F. N. Iandola, M. W. Moskewicz, K. Ashraf, S. Han, W. J. Dally, and K. Keutzer, "Squeezezenet: Alexnet-level accuracy with 50x fewer parameters and <1mb model size," *CoRR*, vol. abs/1602.07360, 2016. [Online]. Available: <http://arxiv.org/abs/1602.07360>

[91] A. G. Howard, M. Zhu, B. Chen, D. Kalenichenko, W. Wang, T. Weyand, M. Andreetto, and H. Adam, "Mobilenets: Efficient convolutional neural networks for mobile vision applications," *CoRR*, vol. abs/1704.04861, 2017. [Online]. Available: <http://arxiv.org/abs/1704.04861>

[92] M. Sandler, A. G. Howard, M. Zhu, A. Zhmoginov, and L. Chen, "Inverted residuals and linear bottlenecks: Mobile networks for classification, detection and segmentation," *CoRR*, vol. abs/1801.04381, 2018. [Online]. Available: <http://arxiv.org/abs/1801.04381>

[93] A. Howard, M. Sandler, G. Chu, L. Chen, B. Chen, M. Tan, W. Wang, Y. Zhu, R. Pang, V. Vasudevan, Q. V. Le, and H. Adam, "Searching for mobilenetv3," *CoRR*, vol. abs/1905.02244, 2019. [Online]. Available: <http://arxiv.org/abs/1905.02244>

[94] X. Zhang, X. Zhou, M. Lin, and J. Sun, "Shufflenet: An extremely efficient convolutional neural network for mobile devices," *CoRR*, vol. abs/1707.01083, 2017. [Online]. Available: <http://arxiv.org/abs/1707.01083>

[95] R. J. Wang, X. Li, S. Ao, and C. X. Ling, "Pelee: A real-time object detection system on mobile devices," *CoRR*, vol. abs/1804.06882, 2018. [Online]. Available: <http://arxiv.org/abs/1804.06882>

[96] N. Ma, X. Zhang, H. Zheng, and J. Sun, "Shufflenet V2: practical guidelines for efficient CNN architecture design," *CoRR*, vol. abs/1807.11164, 2018. [Online]. Available: <http://arxiv.org/abs/1807.11164>

[97] M. Tan, B. Chen, R. Pang, V. Vasudevan, and Q. V. Le, "Mnasnet: Platform-aware neural architecture search for mobile," *CoRR*, vol. abs/1807.11626, 2018. [Online]. Available: <http://arxiv.org/abs/1807.11626>

[98] H. Cai, C. Gan, and S. Han, "Once for all: Train one network and specialize it for efficient deployment," *CoRR*, vol. abs/1908.09791, 2019. [Online]. Available: <http://arxiv.org/abs/1908.09791>

[99] F. Chabot, M. Chaouch, J. Rabarisoa, C. Teuli  re, and T. Chateau, "Deep MANTA: A coarse-to-fine many-task network for joint 2d and 3d vehicle analysis from monocular image," *CoRR*, vol. abs/1703.07570, 2017. [Online]. Available: <http://arxiv.org/abs/1703.07570>

[100] A. Mousavian, D. Anguelov, J. Flynn, and J. Kosecka, "3d bounding box estimation using deep learning and geometry," *CoRR*, vol. abs/1612.00496, 2016. [Online]. Available: <http://arxiv.org/abs/1612.00496>

[101] B. Li, W. Ouyang, L. Sheng, X. Zeng, and X. Wang, "GS3D: an efficient 3d object detection framework for autonomous driving," *CoRR*, vol. abs/1903.10955, 2019. [Online]. Available: <http://arxiv.org/abs/1903.10955>

[102] P. Li, X. Chen, and S. Shen, "Stereo R-CNN based 3d object detection for autonomous driving," *CoRR*, vol. abs/1902.09738, 2019. [Online]. Available: <http://arxiv.org/abs/1902.09738>

[103] X. Shi, Q. Ye, X. Chen, C. Chen, Z. Chen, and T. Kim, "Geometry-based distance decomposition for monocular 3d object detection," *CoRR*, vol. abs/2104.03775, 2021. [Online]. Available: <https://arxiv.org/abs/2104.03775>

[104] X. Ma, Y. Zhang, D. Xu, D. Zhou, S. Yi, H. Li, and W. Ouyang, "Delving into localization errors for monocular 3d object detection," *CoRR*, vol. abs/2103.16237, 2021. [Online]. Available: <https://arxiv.org/abs/2103.16237>

[105] Y. Liu, L. Wang, and M. Liu, "Yolostereo3d: A step back to 2d for efficient stereo 3d detection," *CoRR*, vol. abs/2103.09422, 2021. [Online]. Available: <https://arxiv.org/abs/2103.09422>

[106] T. Yin, X. Zhou, and P. Kr  enb  hl, "Center-based 3d object detection and tracking," *CoRR*, vol. abs/2006.11275, 2020. [Online]. Available: <https://arxiv.org/abs/2006.11275>

[107] Y. Zhou and O. Tuzel, "Voxelnet: End-to-end learning for point cloud based 3d object detection," *CoRR*, vol. abs/1711.06396, 2017. [Online]. Available: <http://arxiv.org/abs/1711.06396>

[108] A. H. Lang, S. Vora, H. Caesar, L. Zhou, J. Yang, and O. Beijbom, "Pointpillars: Fast encoders for object detection from point clouds," *CoRR*, vol. abs/1812.05784, 2018. [Online]. Available: <http://arxiv.org/abs/1812.05784>

[109] Q. Xu, Y. Zhong, and U. Neumann, "Behind the curtain: Learning occluded shapes for 3d object detection," *CoRR*, vol. abs/2112.02205, 2021. [Online]. Available: <https://arxiv.org/abs/2112.02205>

[110] W. Zheng, W. Tang, S. Chen, L. Jiang, and C. Fu, "CIA-SSD: confident iou-aware single-stage object detector from point cloud," *CoRR*, vol. abs/2012.03015, 2020. [Online]. Available: <https://arxiv.org/abs/2012.03015>

[111] W. Zheng, W. Tang, L. Jiang, and C. Fu, "SE-SSD: self-ensembling single-stage object detector from point cloud," *CoRR*, vol. abs/2104.09804, 2021. [Online]. Available: <https://arxiv.org/abs/2104.09804>

[112] J. Deng, S. Shi, P. Li, W. Zhou, Y. Zhang, and H. Li, "Voxel R-CNN: towards high performance voxel-based 3d object detection," *CoRR*, vol. abs/2012.15712, 2020. [Online]. Available: <https://arxiv.org/abs/2012.15712>

[113] H. Sheng, S. Cai, Y. Liu, B. Deng, J. Huang, X. Hua, and M. Zhao, "Improving 3d object detection with channel-wise transformer," *CoRR*, vol. abs/2108.10723, 2021. [Online]. Available: <https://arxiv.org/abs/2108.10723>

[114] J. Mao, Y. Xue, M. Niu, H. Bai, J. Feng, X. Liang, H. Xu, and C. Xu, "Voxel transformer for 3d object detection," *CoRR*, vol. abs/2109.02497, 2021. [Online]. Available: <https://arxiv.org/abs/2109.02497>

[115] S. Vora, A. H. Lang, B. Helou, and O. Beijbom, "Pointpainting: Sequential fusion for 3d object detection," *CoRR*, vol. abs/1911.10150, 2019. [Online]. Available: <http://arxiv.org/abs/1911.10150>

[116] J. Ku, M. Mozifian, J. Lee, A. Harakeh, and S. L. Waslander, "Joint 3d proposal generation and object detection from view aggregation," *CoRR*, vol. abs/1712.02294, 2017. [Online]. Available: <http://arxiv.org/abs/1712.02294>

[117] M. Liang, B. Yang, S. Wang, and R. Urtasun, "Deep continuous fusion for multi-sensor 3d object detection," *CoRR*, vol. abs/2012.10992, 2020. [Online]. Available: <https://arxiv.org/abs/2012.10992>

[118] J. H. Yoo, Y. Kim, J. S. Kim, and J. W. Choi, "3d-cvf: Generating joint camera and lidar features using cross-view spatial feature fusion for 3d object detection," *CoRR*, vol. abs/2004.12636, 2020. [Online]. Available: <https://arxiv.org/abs/2004.12636>

[119] S. Pang, D. Morris, and H. Radha, "Clocs: Camera-lidar object candidates fusion for 3d object detection," *CoRR*, vol. abs/2009.00784, 2020. [Online]. Available: <https://arxiv.org/abs/2009.00784>

[120] L. Ye, M. Rochan, Z. Liu, and Y. Wang, "Cross-modal self-attention network for referring image segmentation," *CoRR*, vol. abs/1904.04745, 2019. [Online]. Available: [http://arxiv.org/abs/1904.04745](https://arxiv.org/abs/1904.04745)

[121] E. Xie, W. Wang, Z. Yu, A. Anandkumar, J. M. Alvarez, and P. Luo, "Segformer: Simple and efficient design for semantic segmentation with transformers," *CoRR*, vol. abs/2105.15203, 2021. [Online]. Available: <https://arxiv.org/abs/2105.15203>

[122] S. Zheng, J. Lu, H. Zhao, X. Zhu, Z. Luo, Y. Wang, Y. Fu, J. Feng, T. Xiang, P. H. S. Torr, and L. Zhang, "Rethinking semantic segmentation from a sequence-to-sequence perspective with transformers," *CoRR*, vol. abs/2012.15840, 2020. [Online]. Available: <https://arxiv.org/abs/2012.15840>

[123] R. Strudel, R. G. Pinel, I. Laptev, and C. Schmid, "Segmenter: Transformer for semantic segmentation," *CoRR*, vol. abs/2105.05633, 2021. [Online]. Available: <https://arxiv.org/abs/2105.05633>

[124] P. Ramachandran, N. Parmar, A. Vaswani, I. Bello, A. Levskaya, and J. Shlens, "Stand-alone self-attention in vision models," *CoRR*, vol. abs/1906.05909, 2019. [Online]. Available: [http://arxiv.org/abs/1906.05909](https://arxiv.org/abs/1906.05909)

[125] W. Wang, E. Xie, X. Li, D. Fan, K. Song, D. Liang, T. Lu, P. Luo, and L. Shao, "Pyramid vision transformer: A versatile backbone for dense prediction without convolutions," *CoRR*, vol. abs/2102.12122, 2021. [Online]. Available: <https://arxiv.org/abs/2102.12122>

[126] A. Kirillov, K. He, R. B. Girshick, C. Rother, and P. Dollár, "Panoptic segmentation," *CoRR*, vol. abs/1801.00868, 2018. [Online]. Available: <http://arxiv.org/abs/1801.00868>

[127] H. Wang, Y. Zhu, B. Green, H. Adam, A. L. Yuille, and L. Chen, "Axial-deeplab: Stand-alone axial-attention for panoptic segmentation," *CoRR*, vol. abs/2003.07853, 2020. [Online]. Available: <https://arxiv.org/abs/2003.07853>

[128] T. Lin, M. Maire, S. J. Belongie, L. D. Bourdev, R. B. Girshick, J. Hays, P. Perona, D. Ramanan, P. Dollár, and C. L. Zitnick, "Microsoft COCO: common objects in context," *CoRR*, vol. abs/1405.0312, 2014. [Online]. Available: <http://arxiv.org/abs/1405.0312>

[129] G. Neuhold, T. Ollmann, S. R. Bulò, and P. Kuntschieder, "The mapillary vistas dataset for semantic understanding of street scenes," in *2017 IEEE International Conference on Computer Vision (ICCV)*, 2017, pp. 5000–5009.

[130] M. Cordts, M. Omran, S. Ramos, T. Rehfeld, M. Enzweiler, R. Benenson, U. Franke, S. Roth, and B. Schiele, "The cityscapes dataset for semantic urban scene understanding," *CoRR*, vol. abs/1604.01685, 2016. [Online]. Available: <http://arxiv.org/abs/1604.01685>

[131] S. Reed, Z. Akata, X. Yan, L. Logeswaran, B. Schiele, and H. Lee, "Generative adversarial text to image synthesis," in *Proceedings of The 33rd International Conference on Machine Learning*, ser. Proceedings of Machine Learning Research, M. F. Balcan and K. Q. Weinberger, Eds., vol. 48. New York, New York, USA: PMLR, 20–22 Jun 2016, pp. 1060–1069. [Online]. Available: <https://proceedings.mlr.press/v48/reed16.html>

[132] H. Zhang, T. Xu, H. Li, S. Zhang, X. Huang, X. Wang, and D. N. Metaxas, "Stackgan: Text to photo-realistic image synthesis with stacked generative adversarial networks," *CoRR*, vol. abs/1612.03242, 2016. [Online]. Available: <http://arxiv.org/abs/1612.03242>

[133] H. Zhang, T. Xu, H. Li, S. Zhang, X. Wang, X. Huang, and D. N. Metaxas, "Stackgan++: Realistic image synthesis with stacked generative adversarial networks," *CoRR*, vol. abs/1710.10916, 2017. [Online]. Available: <http://arxiv.org/abs/1710.10916>

[134] T. Xu, P. Zhang, Q. Huang, H. Zhang, Z. Gan, X. Huang, and X. He, "Attngan: Fine-grained text to image generation with attentional generative adversarial networks," *CoRR*, vol. abs/1711.10485, 2017. [Online]. Available: <http://arxiv.org/abs/1711.10485>

[135] I. J. Goodfellow, J. Pouget-Abadie, M. Mirza, B. Xu, D. Warde-Farley, S. Ozair, A. Courville, and Y. Bengio, "Generative adversarial networks," 2014. [Online]. Available: <https://arxiv.org/abs/1406.2661>

[136] A. Ramesh, M. Pavlov, G. Goh, S. Gray, M. Chen, R. Child, V. Misra, P. Mishkin, G. Krueger, S. Agarwal *et al.*, "Dall-e: Creating images from text," *OpenAI blog*, 2021.

[137] X. Wang, C. Yeshwanth, and M. Nießner, "Sceneformer: Indoor scene generation with transformers," *CoRR*, vol. abs/2012.09793, 2020. [Online]. Available: <https://arxiv.org/abs/2012.09793>

[138] M. Chen, A. Radford, R. Child, J. Wu, H. Jun, D. Luan, and I. Sutskever, "Generative pretraining from pixels," in *Proceedings of the 37th International Conference on Machine Learning*, ser. Proceedings of Machine Learning Research, H. D. III and A. Singh, Eds., vol. 119. PMLR, 13–18 Jul 2020, pp. 1691–1703. [Online]. Available: <https://proceedings.mlr.press/v119/chen20s.html>

[139] P. Esser, R. Rombach, and B. Ommer, "Taming transformers for high-resolution image synthesis," *CoRR*, vol. abs/2012.09841, 2020. [Online]. Available: <https://arxiv.org/abs/2012.09841>

[140] Y. Jiang, S. Chang, and Z. Wang, "Transgan: Two transformers can make one strong GAN," *CoRR*, vol. abs/2102.07074, 2021. [Online]. Available: <https://arxiv.org/abs/2102.07074>

[141] A. K. Bhunia, S. H. Khan, H. Cholakkal, R. M. Anwer, F. S. Khan, and M. Shah, "Handwriting transformers," *CoRR*, vol. abs/2104.03964, 2021. [Online]. Available: <https://arxiv.org/abs/2104.03964>

[142] A. Krizhevsky and G. Hinton, "Learning multiple layers of features from tiny images," University of Toronto, Toronto, Ontario, Tech. Rep. 0, 2009.

[143] A. Coates, A. Ng, and H. Lee, "An analysis of single-layer networks in unsupervised feature learning," in *Proceedings of the Fourteenth International Conference on Artificial Intelligence and Statistics*, ser. Proceedings of Machine Learning Research, G. Gordon, D. Dunson, and M. Dudík, Eds., vol. 15. Fort Lauderdale, FL, USA: PMLR, 11–13 Apr 2011, pp. 215–223. [Online]. Available: <https://proceedings.mlr.press/v15/coates11a.html>

[144] T. Chen, S. Kornblith, M. Norouzi, and G. E. Hinton, "A simple framework for contrastive learning of visual representations," *CoRR*, vol. abs/2002.05709, 2020. [Online]. Available: <https://arxiv.org/abs/2002.05709>

[145] J. Deng, W. Dong, R. Socher, L.-J. Li, K. Li, and L. Fei-Fei, "Imagenet: A large-scale hierarchical image database," in *2009 IEEE Conference on Computer Vision and Pattern Recognition*, 2009, pp. 248–255.

[146] K. He, H. Fan, Y. Wu, S. Xie, and R. B. Girshick, "Momentum contrast for unsupervised visual representation learning," *CoRR*, vol. abs/1911.05722, 2019. [Online]. Available: <http://arxiv.org/abs/1911.05722>

[147] P. Bachman, R. D. Hjelm, and W. Buchwalter, "Learning representations by maximizing mutual information across views," *CoRR*, vol. abs/1906.00910, 2019. [Online]. Available: <http://arxiv.org/abs/1906.00910>

[148] O. J. Hénaff, A. Srinivas, J. D. Fauw, A. Razavi, C. Doersch, S. M. A. Eslami, and A. van den Oord, "Data-efficient image recognition with contrastive predictive coding," *CoRR*, vol.

abs/1905.09272, 2019. [Online]. Available: <http://arxiv.org/abs/1905.09272>

[149] A. Radford, L. Metz, and S. Chintala, "Unsupervised representation learning with deep convolutional generative adversarial networks," *arXiv preprint arXiv:1511.06434*, 2015.

[150] C. Gao, Y. Chen, S. Liu, Z. Tan, and S. Yan, "Adversarialnas: Adversarial neural architecture search for gans," *CoRR*, vol. abs/1912.02037, 2019. [Online]. Available: <http://arxiv.org/abs/1912.02037>

[151] T. Karras, S. Laine, M. Aittala, J. Hellsten, J. Lehtinen, and T. Aila, "Analyzing and improving the image quality of stylegan," *CoRR*, vol. abs/1912.04958, 2019. [Online]. Available: <http://arxiv.org/abs/1912.04958>

[152] F. Yang, H. Yang, J. Fu, H. Lu, and B. Guo, "Learning texture transformer network for image super-resolution," *CoRR*, vol. abs/2006.04139, 2020. [Online]. Available: <https://arxiv.org/abs/2006.04139>

[153] H. Chen, Y. Wang, T. Guo, C. Xu, Y. Deng, Z. Liu, S. Ma, C. Xu, C. Xu, and W. Gao, "Pre-trained image processing transformer," *CoRR*, vol. abs/2012.00364, 2020. [Online]. Available: <https://arxiv.org/abs/2012.00364>

[154] J. Liang, J. Cao, G. Sun, K. Zhang, L. Van Gool, and R. Timofte, "Swinir: Image restoration using swin transformer," 2021. [Online]. Available: <https://arxiv.org/abs/2108.10257>

[155] Z. Wang, X. Cun, J. Bao, and J. Liu, "Uformer: A general u-shaped transformer for image restoration," *CoRR*, vol. abs/2106.03106, 2021. [Online]. Available: <https://arxiv.org/abs/2106.03106>

[156] M. Kumar, D. Weissenborn, and N. Kalchbrenner, "Colorization transformer," *CoRR*, vol. abs/2102.04432, 2021. [Online]. Available: <https://arxiv.org/abs/2102.04432>

[157] S. Antol, A. Agrawal, J. Lu, M. Mitchell, D. Batra, C. L. Zitnick, and D. Parikh, "VQA: visual question answering," *CoRR*, vol. abs/1505.00468, 2015. [Online]. Available: <http://arxiv.org/abs/1505.00468>

[158] R. Zellers, Y. Bisk, A. Farhadi, and Y. Choi, "From recognition to cognition: Visual commonsense reasoning," *CoRR*, vol. abs/1811.10830, 2018. [Online]. Available: <http://arxiv.org/abs/1811.10830>

[159] K. Lee, X. Chen, G. Hua, H. Hu, and X. He, "Stacked cross attention for image-text matching," *CoRR*, vol. abs/1803.08024, 2018. [Online]. Available: <http://arxiv.org/abs/1803.08024>

[160] O. Vinyals, A. Toshev, S. Bengio, and D. Erhan, "Show and tell: A neural image caption generator," *CoRR*, vol. abs/1411.4555, 2014. [Online]. Available: <http://arxiv.org/abs/1411.4555>

[161] Y. Chen, L. Li, L. Yu, A. E. Kholy, F. Ahmed, Z. Gan, Y. Cheng, and J. Liu, "UNITER: learning universal image-text representations," *CoRR*, vol. abs/1909.11740, 2019. [Online]. Available: <http://arxiv.org/abs/1909.11740>

[162] X. Li, X. Yin, C. Li, P. Zhang, X. Hu, L. Zhang, L. Wang, H. Hu, L. Dong, F. Wei, Y. Choi, and J. Gao, "Oscar: Object-semantics aligned pre-training for vision-language tasks," *CoRR*, vol. abs/2004.06165, 2020. [Online]. Available: <https://arxiv.org/abs/2004.06165>

[163] C. Sun, A. Myers, C. Vondrick, K. Murphy, and C. Schmid, "Videobert: A joint model for video and language representation learning," *CoRR*, vol. abs/1904.01766, 2019. [Online]. Available: <http://arxiv.org/abs/1904.01766>

[164] G. Li, N. Duan, Y. Fang, D. Jiang, and M. Zhou, "Unicoder-vl: A universal encoder for vision and language by cross-modal pre-training," *CoRR*, vol. abs/1908.06066, 2019. [Online]. Available: <http://arxiv.org/abs/1908.06066>

[165] L. H. Li, M. Yatskar, D. Yin, C. Hsieh, and K. Chang, "Visualbert: A simple and performant baseline for vision and language," *CoRR*, vol. abs/1908.03557, 2019. [Online]. Available: <http://arxiv.org/abs/1908.03557>

[166] W. Su, X. Zhu, Y. Cao, B. Li, L. Lu, F. Wei, and J. Dai, "VL-BERT: pre-training of generic visual-linguistic representations," *CoRR*, vol. abs/1908.08530, 2019. [Online]. Available: <http://arxiv.org/abs/1908.08530>

[167] H. Tan and M. Bansal, "LXMERT: learning cross-modality encoder representations from transformers," *CoRR*, vol. abs/1908.07490, 2019. [Online]. Available: <http://arxiv.org/abs/1908.07490>

[168] J. Lu, D. Batra, D. Parikh, and S. Lee, "Vilbert: Pretraining task-agnostic visiolinguistic representations for vision-and-language tasks," *CoRR*, vol. abs/1908.02265, 2019. [Online]. Available: <http://arxiv.org/abs/1908.02265>

[169] S. Lee, Y. Yu, G. Kim, T. M. Breuel, J. Kautz, and Y. Song, "Parameter efficient multimodal transformers for video representation learning," *CoRR*, vol. abs/2012.04124, 2020. [Online]. Available: <https://arxiv.org/abs/2012.04124>

[170] N. Sun, Y. Zhu, and X. Hu, "Faster r-cnn based table detection combining corner locating," *2019 International Conference on Document Analysis and Recognition (ICDAR)*, pp. 1314–1319, 2019.

[171] N. Parmar, A. Vaswani, J. Uszkoreit, L. Kaiser, N. Shazeer, and A. Ku, "Image transformer," *CoRR*, vol. abs/1802.05751, 2018. [Online]. Available: <http://arxiv.org/abs/1802.05751>

[172] I. Bello, B. Zoph, A. Vaswani, J. Shlens, and Q. V. Le, "Attention augmented convolutional networks," *CoRR*, vol. abs/1904.09925, 2019. [Online]. Available: <http://arxiv.org/abs/1904.09925>

[173] S. H. Rezatofighi, N. Tsoi, J. Gwak, A. Sadeghian, I. D. Reid, and S. Savarese, "Generalized intersection over union: A metric and A loss for bounding box regression," *CoRR*, vol. abs/1902.09630, 2019. [Online]. Available: <http://arxiv.org/abs/1902.09630>

[174] A. van den Oord, Y. Li, I. Babuschkin, K. Simonyan, O. Vinyals, K. Kavukcuoglu, G. van den Driessche, E. Lockhart, L. C. Cobo, F. Stimberg, N. Casagrande, D. Grawe, S. Noury, S. Dieleman, E. Elsen, N. Kalchbrenner, H. Zen, A. Graves, H. King, T. Walters, D. Belov, and D. Hassabis, "Parallel wavenet: Fast high-fidelity speech synthesis," *CoRR*, vol. abs/1711.10433, 2017. [Online]. Available: <http://arxiv.org/abs/1711.10433>

[175] J. Gu, J. Bradbury, C. Xiong, V. O. K. Li, and R. Socher, "Non-autoregressive neural machine translation," *CoRR*, vol. abs/1711.02281, 2017. [Online]. Available: <http://arxiv.org/abs/1711.02281>

[176] M. Ghazvininejad, O. Levy, Y. Liu, and L. Zettlemoyer, "Mask-predict: Parallel decoding of conditional masked language models," *arXiv preprint arXiv:1904.09324*, 2019.

[177] R. Stewart and M. Andriluka, "End-to-end people detection in crowded scenes," *CoRR*, vol. abs/1506.04878, 2015. [Online]. Available: <http://arxiv.org/abs/1506.04878>

[178] B. Romera-Paredes and P. H. S. Torr, "Recurrent instance segmentation," *CoRR*, vol. abs/1511.08250, 2015. [Online]. Available: <http://arxiv.org/abs/1511.08250>

[179] E. Park and A. C. Berg, "Learning to decompose for object detection and instance segmentation," *CoRR*, vol. abs/1511.06449, 2015. [Online]. Available: <http://arxiv.org/abs/1511.06449>

[180] M. Ren and R. S. Zemel, "End-to-end instance segmentation and counting with recurrent attention," *CoRR*, vol. abs/1605.09410, 2016. [Online]. Available: <http://arxiv.org/abs/1605.09410>

[181] A. Salvador, M. Bellver, M. Baradad, F. Marqués, J. Torres, and X. Giró-i-Nieto, "Recurrent neural networks for semantic instance segmentation," *CoRR*, vol. abs/1712.00617, 2017. [Online]. Available: <http://arxiv.org/abs/1712.00617>

[182] J. Dai, H. Qi, Y. Xiong, Y. Li, G. Zhang, H. Hu, and Y. Wei, "Deformable convolutional networks," *CoRR*, vol. abs/1703.06211, 2017. [Online]. Available: <http://arxiv.org/abs/1703.06211>

[183] X. Zhu, H. Hu, S. Lin, and J. Dai, "Deformable convnets v2: More deformable, better results," *CoRR*, vol. abs/1811.11168, 2018. [Online]. Available: <http://arxiv.org/abs/1811.11168>

[184] H. Zhang and J. Wang, "Towards adversarially robust object detection," *CoRR*, vol. abs/1907.10310, 2019. [Online]. Available: <http://arxiv.org/abs/1907.10310>

[185] Y. Wu, Y. Chen, L. Yuan, Z. Liu, L. Wang, H. Li, and Y. Fu, "Rethinking classification and localization in R-CNN," *CoRR*, vol. abs/1904.06493, 2019. [Online]. Available: <http://arxiv.org/abs/1904.06493>

[186] G. Song, Y. Liu, and X. Wang, "Revisiting the sibling head in object detector," *CoRR*, vol. abs/2003.07540, 2020. [Online]. Available: <https://arxiv.org/abs/2003.07540>

[187] L. Dong, N. Yang, W. Wang, F. Wei, X. Liu, Y. Wang, J. Gao, M. Zhou, and H. Hon, "Unified language model pre-training for natural language understanding and generation," *CoRR*, vol. abs/1905.03197, 2019. [Online]. Available: <http://arxiv.org/abs/1905.03197>

[188] N. Srivastava, G. Hinton, A. Krizhevsky, I. Sutskever, and R. Salakhutdinov, "Dropout: A simple way to prevent neural networks from overfitting," *Journal of Machine Learning Research*, vol. 15, no. 56, pp. 1929–1958, 2014. [Online]. Available: <http://jmlr.org/papers/v15/srivastava14a.html>

[189] P. Sun, R. Zhang, Y. Jiang, T. Kong, C. Xu, W. Zhan, M. Tomizuka, L. Li, Z. Yuan, C. Wang, and P. Luo, "Sparse R-CNN: end-to-end object detection with learnable proposals," *CoRR*, vol. abs/2011.12450, 2020. [Online]. Available: <https://arxiv.org/abs/2011.12450>

[190] X. Zhang, F. Wan, C. Liu, R. Ji, and Q. Ye, "Freeanchor: Learning to match anchors for visual object detection," *CoRR*, vol. abs/1909.02466, 2019. [Online]. Available: <http://arxiv.org/abs/1909.02466>

[191] K. Kim and H. S. Lee, "Probabilistic anchor assignment with iou prediction for object detection," *CoRR*, vol. abs/2007.08103, 2020. [Online]. Available: <https://arxiv.org/abs/2007.08103>

[192] H. Li, Z. Wu, C. Zhu, C. Xiong, R. Socher, and L. S. Davis, "Learning from noisy anchors for one-stage object detection," *CoRR*, vol. abs/1912.05086, 2019. [Online]. Available: <http://arxiv.org/abs/1912.05086>

[193] Z. Tian, C. Shen, H. Chen, and T. He, "Fcos: Fully convolutional one-stage object detection," in *2019 IEEE/CVF International Conference on Computer Vision (ICCV)*, 2019, pp. 9626–9635.

[194] S. Ren, K. He, R. B. Girshick, and J. Sun, "Faster R-CNN: towards real-time object detection with region proposal networks," *CoRR*, vol. abs/1506.01497, 2015. [Online]. Available: <http://arxiv.org/abs/1506.01497>

[195] Y. Wu and K. He, "Group normalization," *CoRR*, vol. abs/1803.08494, 2018. [Online]. Available: <http://arxiv.org/abs/1803.08494>

[196] Y. Chen, Y. Kalantidis, J. Li, S. Yan, and J. Feng, "A²-nets: Double attention networks," *CoRR*, vol. abs/1810.11579, 2018. [Online]. Available: <http://arxiv.org/abs/1810.11579>

[197] T.-Y. Lin, A. RoyChowdhury, and S. Maji, "Bilinear cnn models for fine-grained visual recognition," in *2015 IEEE International Conference on Computer Vision (ICCV)*, 2015, pp. 1449–1457.

[198] X. Wang, S. Zhang, Z. Yu, L. Feng, and W. Zhang, "Scale-equalizing pyramid convolution for object detection," *2020 IEEE/CVF Conference on Computer Vision and Pattern Recognition (CVPR)*, pp. 13 356–13 365, 2020.

[199] J. Hu, L. Shen, and G. Sun, "Squeeze-and-excitation networks," *CoRR*, vol. abs/1709.01507, 2017. [Online]. Available: <http://arxiv.org/abs/1709.01507>

[200] Y. Chen, X. Dai, M. Liu, D. Chen, L. Yuan, and Z. Liu, "Dynamic relu," in *Computer Vision – ECCV 2020*, A. Vedaldi, H. Bischof, T. Brox, and J.-M. Frahm, Eds. Cham: Springer International Publishing, 2020, pp. 351–367.

[201] X. Dai, Y. Chen, B. Xiao, D. Chen, M. Liu, L. Yuan, and L. Zhang, "Dynamic head: Unifying object detection heads with attentions," *CoRR*, vol. abs/2106.08322, 2021. [Online]. Available: <https://arxiv.org/abs/2106.08322>

[202] Z. Jiang, W. Yu, D. Zhou, Y. Chen, J. Feng, and S. Yan, "Convbert: Improving BERT with span-based dynamic convolution," *CoRR*, vol. abs/2008.02496, 2020. [Online]. Available: <https://arxiv.org/abs/2008.02496>

[203] J. Beal, E. Kim, E. Tzeng, D. H. Park, A. Zhai, and D. Kislyuk, "Toward transformer-based object detection," *CoRR*, vol. abs/2012.09958, 2020. [Online]. Available: <https://arxiv.org/abs/2012.09958>

[204] B. Zhu, J. Wang, Z. Jiang, F. Zong, S. Liu, Z. Li, and J. Sun, "Autoassign: Differentiable label assignment for dense object detection," *CoRR*, vol. abs/2007.03496, 2020. [Online]. Available: <https://arxiv.org/abs/2007.03496>

[205] D. Hendrycks and K. Gimpel, "Bridging nonlinearities and stochastic regularizers with gaussian error linear units," *CoRR*, vol. abs/1606.08415, 2016. [Online]. Available: <https://arxiv.org/abs/1606.08415>

[206] J. L. Ba, J. R. Kiros, and G. E. Hinton, "Layer normalization," 2016. [Online]. Available: <https://arxiv.org/abs/1607.06450>

[207] X. Ma, X. Kong, S. Wang, C. Zhou, J. May, H. Ma, and L. Zettlemoyer, "Luna: Linear unified nested attention," *CoRR*, vol. abs/2106.01540, 2021. [Online]. Available: <https://arxiv.org/abs/2106.01540>

[208] Z. Shen, M. Zhang, S. Yi, J. Yan, and H. Zhao, "Factorized attention: Self-attention with linear complexities," *CoRR*, vol. abs/1812.01243, 2018. [Online]. Available: <http://arxiv.org/abs/1812.01243>

[209] Z. Ge, S. Liu, F. Wang, Z. Li, and J. Sun, "YOLOX: exceeding YOLO series in 2021," *CoRR*, vol. abs/2107.08430, 2021. [Online]. Available: <https://arxiv.org/abs/2107.08430>

[210] D. M. W. Powers, "Evaluation: from precision, recall and f-measure to roc, informedness, markedness and correlation," *CoRR*, vol. abs/2010.16061, 2020. [Online]. Available: <https://arxiv.org/abs/2010.16061>

[211] H. Touvron, M. Cord, M. Douze, F. Massa, A. Sablayrolles, and H. Jégou, "Training data-efficient image transformers & distillation through attention," *CoRR*, vol. abs/2012.12877, 2020. [Online]. Available: <https://arxiv.org/abs/2012.12877>

[212] Z. Liu, Y. Lin, Y. Cao, H. Hu, Y. Wei, Z. Zhang, S. Lin, and B. Guo, "Swin transformer: Hierarchical vision transformer using shifted windows," *CoRR*, vol. abs/2103.14030, 2021. [Online]. Available: <https://arxiv.org/abs/2103.14030>